Karlsruhe Institute of Technology

Wave phenomena
analysis and numerics

Error analysis of a second order locally implicit method for linear Maxwell's equations

Marlis Hochbruck, Andreas Sturm

CRC Preprint 2015/1, September 2015

KARLSRUHE INSTITUTE OF TECHNOLOGY

CRC 1173

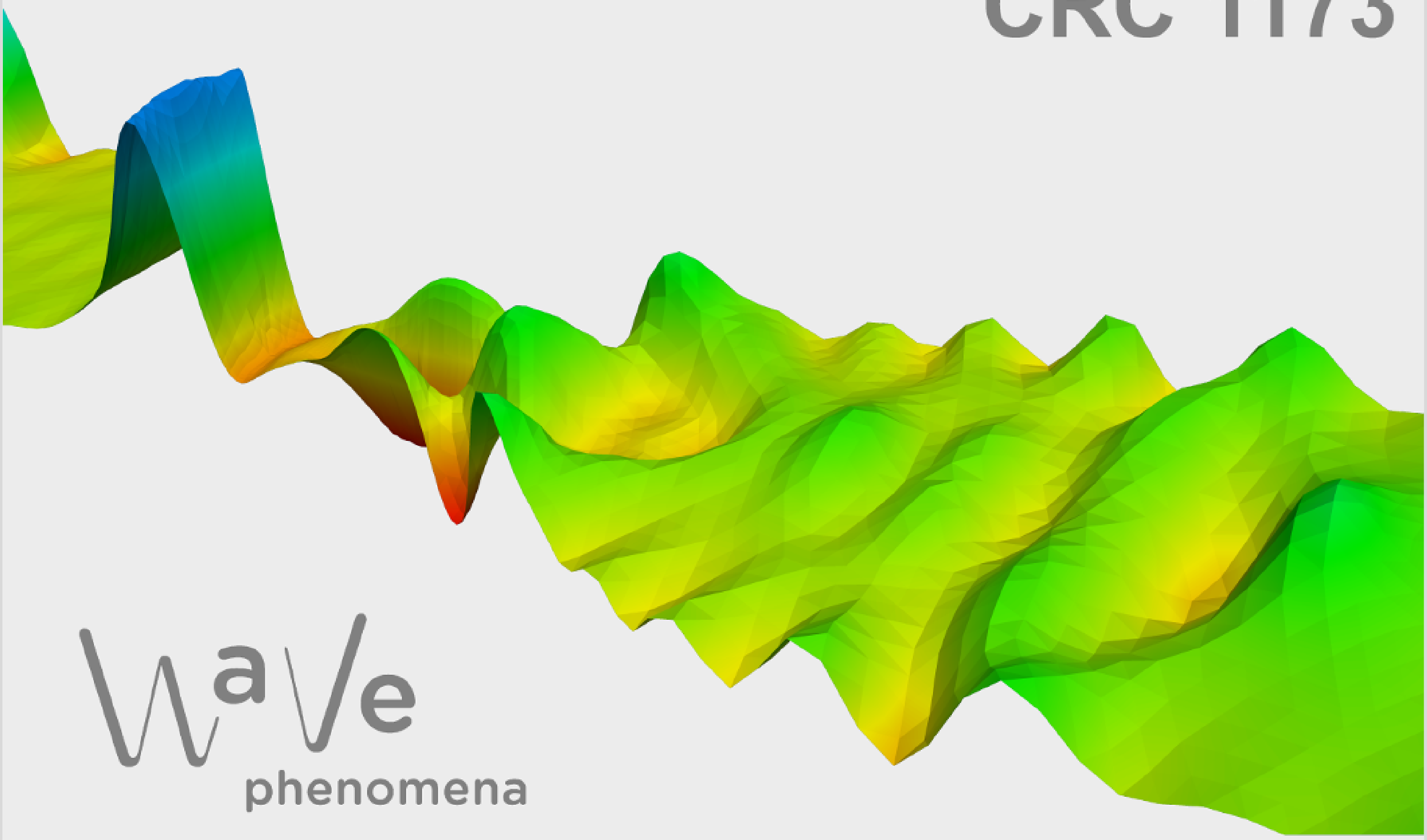

Wave phenomena

Participating universities

Universität Stuttgart

EBERHARD KARLS
UNIVERSITÄT
TÜBINGEN

Funded by

DFG

ISSN 2365-662X

ERROR ANALYSIS OF A SECOND ORDER LOCALLY IMPLICIT METHOD FOR LINEAR MAXWELL'S EQUATIONS*

MARLIS HOCHBRUCK, AND ANDREAS STURM†

Abstract.
In this paper we consider the full discretization of linear Maxwell's equations on spatial grids which are locally refined. For such problems, explicit time integration schemes become inefficient because the smallest mesh width results in a strict CFL condition. Recently locally implicit time integration methods have become popular in overcoming the problem of so called grid-induced stiffness. Various such schemes have been proposed in the literature and have been shown to be very efficient. However, a rigorous analysis of such methods is still missing. In fact, the available literature focuses on error bounds which are valid on a fixed spatial mesh only but deteriorate in the limit where the smallest spatial mesh size tends to zero. Moreover, some important questions cannot be answered without such an analysis. For example, it has not yet been studied which elements of the spatial mesh enter the CFL condition.

In this paper we provide such a rigorous analysis for a locally implicit scheme proposed by Verwer [15] based on a variational formulation and energy techniques.

Key words. Locally implicit methods, component splitting, time integration, discontinuous Galerkin finite elements, error analysis, evolution equations, Maxwell's equations, energy techniques.

AMS subject classifications. Primary: 65M12, 65M15. Secondary: 65M60, 65J10.

1. Introduction. An attractive feature of discontinuous Galerkin (dG) spatial discretizations of Maxwell's equations (cf. the textbooks [4, 9]) is their ability to handle complex geometries by using unstructured, possibly locally-refined meshes. Furthermore, they are well-adapted to handle composite media with varying material coefficients and thus varying speeds of light. In addition, dG methods lead to block diagonal mass matrices which in combination with an explicit time integration method allow for a fully explicit scheme. However, such explicit approaches suffer from a severe restriction of the time step size τ due to stability, the well-known CFL condition, because of the grid induced stiffness of the ode. For Maxwell's equations, we have $\tau \lesssim c_\infty^{-1} h_{\min}$, where $h_{\min}$ denotes the smallest diameter of the elements of the mesh and c_∞ the maximum speed of light. In the case where only a few of the mesh elements have a very small diameter or give rise to a huge speed of light but the major part of the spatial domain contains rather coarse elements or materials with a moderate speed of light this restriction makes the simulation inefficient: One has to do many tiny time steps which then lead to a temporal error which is considerably smaller than the spatial error. A natural way to overcome this restriction is obtained by using implicit time integrators but at the expense of having to solve a large linear system each time step. Alternatively, one can combine an explicit and an implicit scheme by treating only the tiny mesh elements implicitly while retaining an explicit time integration for the remaining elements. This results in so called locally implicit methods which have been considered in [2, 3, 5, 12, 14, 15]. An alternative is to use local timestepping methods, cf. [1, 6, 7, 8], for instance.

In this paper we present a rigorous error analysis of the full discretization of the linear Maxwell's equations using dG discretizations in space and a second-order

*We gratefully acknowledge financial support by the Deutsche Forschungsgemeinschaft (DFG) through RTG 1294 and CRC 1173.

†Institute for Applied and Numerical Analysis, Karlsruhe Institute of Technology, 76128 Karlsruhe, Germany, marlis.hochbruck@kit.edu, andreas.sturm@kit.edu

locally implicit scheme comprising the Crank–Nicolson and the Verlet method for the time integration. This method was proposed and analyzed by Verwer [15] for the ode resulting from spatial discretization. Related methods are considered in [2, 3, 14]. As a byproduct, our error analysis also provides error bounds for the original Crank–Nicolson and the Verlet method, respectively.

For the locally implicit scheme we provide a construction of the splitting between fine and coarse elements. This was not considered in the previous work [2, 3, 15], which suggested a component splitting based on the matrices of the ode system. Using a variational formulation of the evolution equation our analysis shows that it is not sufficient to treat only the fine elements implicitly but also their direct neighbors. Moreover, the split operators have to be chosen with care to inherit certain properties of the continuous operators. We then prove that the method

(a) is stable under a CFL condition which only depends on the coarse elements and
(b) it converges of order two in the time step and k in the space discretization parameter for dG with central fluxes and polynomials of degree k.

The proof of stability uses a particular representation of the operators involved which enables us to make use of properties of the discrete split operators. The techniques used for the error analysis are based on our work [10] for fully implicit Runge–Kutta discretizations of the linear Maxwell's equations.

The paper is organized as follows. In Section 2 we present the analytic and discrete setting of Maxwell's equations and their dG spatial discretization. In particular we construct the splitting of the discretized operators. The proofs of this section are collected in the appendix. Section 3 deals with time integration. We recall the locally implicit scheme by Verwer and generalize it to the variational formulation resulting from the dG discretization. In Section 4 we prove the stability of the scheme and in Section 5 we present our main result (Theorem 5.2). Section 6 contains numerical experiments to illustrate the theoretical result. A careful study of the computational efficiency of such methods compared with other approaches is without the scope of this paper but will be presented elsewhere. Finally, Section 7 contains some concluding remarks.

2. Maxwell's equations and their spatial discretization using dG methods. In this section we state the problem and the notation and review the dG discretization. Since the focus of this paper is on time integration and the results can be proven with standard dG techniques, all proofs are postponed to the appendix.

2.1. Analytic setting. Let Ω be an open, bounded Lipschitz domain in $\mathbb{R}^d$, $d = 1, 2, 3$, and let $T > 0$ be a finite time. The linear Maxwell's equations in a composite medium with permeability $\mu : \Omega \to \mathbb{R}$, permittivity $\varepsilon : \Omega \to \mathbb{R}$ and a perfectly conduction boundary are given by

$$\begin{aligned}
\mu\partial_t \mathbf{H} &= -\operatorname{curl} \mathbf{E}, && (0,T)\times\Omega,\\
\varepsilon\partial_t \mathbf{E} &= \operatorname{curl} \mathbf{H} - \mathbf{J}, && (0,T)\times\Omega,\\
\mathbf{H}(0) &= \mathbf{H}^0, \quad \mathbf{E}(0) = \mathbf{E}^0, && \Omega,\\
n \times \mathbf{E} &= 0, && (0,T)\times\partial\Omega.
\end{aligned} \tag{2.1}$$

Here, $\mathbf{H}, \mathbf{E} : (0,T) \times \Omega \to \mathbb{R}^d$ are the magnetic and electric field, respectively, and $\mathbf{J} : (0,T) \times \Omega \to \mathbb{R}^d$ is the electric current density. Furthermore, n denotes the unit outer normal vector of the domain Ω. The system (2.1) is complemented with the so called divergence conditions

$$\operatorname{div}(\mu\mathbf{H}) = 0, \qquad \operatorname{div}(\varepsilon\mathbf{E}) = \rho, \qquad (0,T)\times\Omega, \tag{2.2}$$

and the boundary condition

$$n\cdot(\mu\mathbf{H}) = 0, \qquad (0,T)\times\partial\Omega. \tag{2.3}$$

Thereby, $\rho : (0,T)\times\Omega \to \mathbb{R}$ is the electric charge density. We assume that it is connected to the electric current density $\mathbf{J}$ via

$$\operatorname{div}\mathbf{J} + \partial_t\rho = 0, \tag{2.4}$$

since then it is well-known [11] that if the divergence conditions (2.2) are satisfied at the initial time $t = 0$ they will be satisfied for every time $t > 0$. Since the same holds true for the boundary condition (2.3) it is sufficient to ensure that the initial values $\mathbf{H}^0$ and $\mathbf{E}^0$ satisfy conditions (2.2) and (2.3) and then only consider the system (2.1).

Further, we assume

$$\mu,\varepsilon \in L^\infty(\Omega), \qquad \mu > \mu_0 > 0, \qquad \varepsilon > \varepsilon_0 > 0. \tag{2.5}$$

We can write (2.1) as the Cauchy problem

$$\partial_t\mathbf{H}(t) = -\mathcal{C}_\mathbf{E}\mathbf{E}(t), \tag{2.6a}$$

$$\partial_t\mathbf{E}(t) = \mathcal{C}_\mathbf{H}\mathbf{H}(t) - \varepsilon^{-1}\mathbf{J}(t), \tag{2.6b}$$

$$\mathbf{H}(0) = \mathbf{H}^0, \quad \mathbf{E}(0) = \mathbf{E}^0, \tag{2.6c}$$

or equivalently for $\mathbf{u} = (\mathbf{H},\mathbf{E})$ and $\mathbf{j} = (0, -\varepsilon^{-1}\mathbf{J})$

$$\partial_t\mathbf{u}(t) = \mathcal{C}\mathbf{u}(t) + \mathbf{j}(t), \qquad \mathbf{u}(0) = \mathbf{u}^0. \tag{2.6d}$$

Here, the Maxwell operator

$$\mathcal{C} = \begin{pmatrix} 0 & -\mathcal{C}_\mathbf{E} \\ \mathcal{C}_\mathbf{H} & 0 \end{pmatrix} = \begin{pmatrix} 0 & -\mu^{-1}\operatorname{curl} \\ \varepsilon^{-1}\operatorname{curl} & 0 \end{pmatrix} \tag{2.7}$$

is defined on its domain $D(\mathcal{C}) = D(\mathcal{C}_\mathbf{H})\times D(\mathcal{C}_\mathbf{E}) = H(\operatorname{curl},\Omega)\times H_0(\operatorname{curl},\Omega)$.

For a set $K\subset\Omega$ and vector fields $\mathbf{U},\widehat{\mathbf{U}},\mathbf{V},\widehat{\mathbf{V}}$ (in $\mathbb{R}^d$) we denote the $L^2(K)$-inner product by

$$\big(\mathbf{U},\widehat{\mathbf{U}}\big)_K = \int_K \mathbf{U}\cdot\widehat{\mathbf{U}}\,dx, \tag{2.8}$$

and for $F\subset\partial K$ we write

$$\big(\mathbf{U},\widehat{\mathbf{U}}\big)_F = \int_F \mathbf{U}|_F\cdot\widehat{\mathbf{U}}|_F\,d\sigma. \tag{2.9}$$

Let $\mathbf{u} = (\mathbf{U},\mathbf{V})$ and $\widehat{\mathbf{u}} = (\widehat{\mathbf{U}},\widehat{\mathbf{V}})$. Given uniformly positive weight functions $\alpha,\beta : \Omega\to\mathbb{R}_{>0}$ we write the weighted inner products as

$$\big(\mathbf{U},\widehat{\mathbf{U}}\big)_{\alpha,K} = \big(\alpha\mathbf{U},\widehat{\mathbf{U}}\big)_K, \qquad \big(\mathbf{u},\widehat{\mathbf{u}}\big)_{\alpha\times\beta,K} = \big(\mathbf{U},\widehat{\mathbf{U}}\big)_{\alpha,K} + \big(\mathbf{V},\widehat{\mathbf{V}}\big)_{\beta,K}. \tag{2.10}$$

By $\|\cdot\|_\alpha$ and $\|\cdot\|_{\alpha\times\beta}$ we denote the corresponding norms. We abbreviate $\big(\cdot,\cdot\big) = \big(\cdot,\cdot\big)_\Omega$ and $\|\cdot\| = \|\cdot\|_\Omega$ and analogously for the weighted inner products and norms.

It is well-known that the Maxwell operator $\mathcal{C}$ is skew-adjoint w.r.t. $\big(\cdot,\cdot\big)_{\mu\times\varepsilon}$ which can be expressed in terms of the curl-operators $\mathcal{C}_{\mathbf{H}}$, $\mathcal{C}_{\mathbf{E}}$ as

$$\big(\mathcal{C}_{\mathbf{H}}\mathbf{H},\mathbf{E}\big)_\varepsilon = \big(\mathbf{H},\mathcal{C}_{\mathbf{E}}\mathbf{E}\big)_\mu, \qquad \mathbf{H} \in D(\mathcal{C}_{\mathbf{H}}),\ \mathbf{E} \in D(\mathcal{C}_{\mathbf{E}}). \tag{2.11}$$

For vanishing source term $\mathbf{J}(t)$ the solution $(\mathbf{H}(t),\mathbf{E}(t))$ of (2.6) conserves the electromagnetic energy

$$\mathcal{E}(\mathbf{H},\mathbf{E}) = \frac{1}{2}\Big(\|\mathbf{H}\|_\mu^2 + \|\mathbf{E}\|_\varepsilon^2\Big), \tag{2.12}$$

i.e., $\mathcal{E}\big(\mathbf{H}(t),\mathbf{E}(t)\big) = \mathcal{E}\big(\mathbf{H}^0,\mathbf{E}^0\big)$ for $t \geq 0$.

Last, we point out that by Stone's theorem [13, Theorem 1.10.8], for initial values $\mathbf{u}^0 = (\mathbf{H}^0,\mathbf{E}^0) \in D(\mathcal{C})$ and source term $\mathbf{J}$ satisfying $\mathbf{J} \in C^1(0,T;L^2(\Omega)^3)$ or $\mathbf{J} \in C(0,T;D(\mathcal{C}_{\mathbf{E}}))$ [13, Corollaries 2.5, 2.6] there exists a unique solution $\mathbf{u}(t) = (\mathbf{H}(t),\mathbf{E}(t)) \in C^1(0,T;L^2(\Omega)^6) \cap C(0,T;D(\mathcal{C}))$ of (2.6) which is bounded by

$$\|\mathbf{u}(t)\|_{\mu\times\varepsilon} \leq \|\mathbf{u}^0\|_{\mu\times\varepsilon} + \int_0^t \|\mathbf{J}(s)\|\ ds. \tag{2.13}$$

2.2. Discrete setting. We discretize (2.6) in space by using a dG method, see [4, 9]. For the sake of readability we restrict ourselves to simplicial meshes. However, all results also hold for more general meshes which are shape and contact regular, cf. [4, Section 1.4]. Moreover, we assume that Ω is approximated by a polyhedron in $\mathbb{R}^d$ which we denote by Ω again, for simplicity.

We use the following notation: By $\mathbb{P}_k$ we denote the set of polynomials of degree at most k. Ω is equipped with a mesh $\mathcal{T}_h = \{K\}$ with elements K. The diameter of an element K is denoted by h_K and the maximal diameter is written as $h_{\max} = \max_{K\in\mathcal{T}_h} h_K$. Moreover, the faces $\mathcal{F}_h$ of $\mathcal{T}_h$ are decomposed into interior and boundary faces: $\mathcal{F}_h = \mathcal{F}_h^{\text{int}} \cup \mathcal{F}_h^{\text{bnd}}$. The maximum number of mesh faces composing the boundary of a mesh element is denoted by N_∂,

$$N_\partial = \max_{K\in\mathcal{T}_h} \operatorname{card}\{F \in \mathcal{F}_h \mid F \subset \partial K\}.$$

For simplicial meshes N_∂ is a constant (e.g., $N_\partial = 3$ for triangular meshes). For every interior face $F \in \mathcal{F}_h^{\text{int}}$ we choose arbitrarily one of the outer unit normals of the two mesh elements composing the face F. We fix this normal and denote it with n_F. We use the notation K and K_F for two neighboring elements $\partial K \cap \partial K_F = F \in \mathcal{F}_h^{\text{int}}$ whereby the unit normal n_F points from K to K_F. For a boundary face the orientation of n_F is always outwards.

The dG space w.r.t. $\mathcal{T}_h$ and piecewise polynomials of degree k is defined as

$$V_h = \big\{v_h \in L^2(\Omega) \mid v_h|_K \in \mathbb{P}_k(K) \text{ for all } K \in \mathcal{T}_h\big\}^3. \tag{2.14}$$

In general, we have $V_h \times V_h \not\subset D(\mathcal{C})$, thus the method is non-conforming. We denote the broken Sobolev spaces by

$$H^q(\mathcal{T}_h) = \big\{v \in L^2(\Omega) \mid v|_K \in H^q(K) \text{ for all } K \in \mathcal{T}_h\big\}, \qquad q \in \mathbb{N}. \tag{2.15}$$

$H^q(\mathcal{T}_h)$ is a Hilbert space with seminorm and norm

$$|v|_q^2 = \sum_{K\in\mathcal{T}_h} |v|_{q,K}^2 = \sum_{K\in\mathcal{T}_h} |v|_{H^q(K)}^2, \qquad \|v\|_q^2 = \sum_{j=0}^{q} |v|_j^2, \tag{2.16}$$

respectively.

ASSUMPTION 2.1. *We suppose that the coefficients μ and ε are piecewise constant and that the mesh $\mathcal{T}_h$ is matched to them such that $\mu_K = \mu|_K$ and $\varepsilon_K = \varepsilon|_K$ are constant for each $K \in \mathcal{T}_h$.*

The L^2-orthogonal projection $\pi_h : L^2(\Omega)^3 \to V_h$ onto V_h is defined such that for $\mathbf{V} \in L^2(\Omega)^3$

$$\big(\mathbf{V} - \pi_h\mathbf{V}, \varphi_h\big) = 0 \qquad \text{for all} \quad \varphi_h \in V_h. \tag{2.17}$$

For piecewise constant coefficients we then have

$$\big(\mathbf{V} - \pi_h\mathbf{V}, \varphi_h\big)_\mu = \big(\mathbf{V} - \pi_h\mathbf{V}, \varphi_h\big)_\varepsilon = 0, \qquad \text{for all} \quad \varphi_h \in V_h. \tag{2.18}$$

Given a piecewise constant weight function α, i.e., $\alpha|_K = \alpha_K$ for all $K \in \mathcal{T}_h$, the weighted average of a function v over an interior face $F \in \mathcal{F}_h^{\mathrm{int}}$ w.r.t. α is defined as

$$\{\!\{v\}\!\}_F^\alpha = \frac{\alpha_K (v|_K)|_F + \alpha_{K_F} (v|_{K_F})|_F}{\alpha_K + \alpha_{K_F}}, \tag{2.19}$$

and the jump of v over F as

$$[\![v]\!]_F = (v|_{K_F})|_F - (v|_K)|_F. \tag{2.20}$$

For vector fields these operations act componentwise.

2.3. Discretization of the curl operators. We denote by $c = (\mu\varepsilon)^{-1/2}$ the speed of light. Given $\mathbf{H}_h, \mathbf{E}_h \in V_h$ and $\phi_h, \psi_h \in V_h$ we define the central fluxes dG discretization of the curl operators $\mathcal{C}_\mathbf{H}$, $\mathcal{C}_\mathbf{E}$ by

$$\big(\boldsymbol{\mathcal{C}}_\mathbf{H}\mathbf{H}_h, \psi_h\big)_\varepsilon = \sum_{K\in\mathcal{T}_h} \big(\operatorname{curl}\mathbf{H}_h, \psi_h\big)_K + \sum_{F\in\mathcal{F}_h^{\mathrm{int}}} \big(n_F \times [\![\mathbf{H}_h]\!]_F, \{\!\{\psi_h\}\!\}_F^{\varepsilon c}\big)_F\ , \tag{2.21a}$$

and

$$\begin{aligned}\big(\boldsymbol{\mathcal{C}}_\mathbf{E}\mathbf{E}_h, \phi_h\big)_\mu = &\sum_{K\in\mathcal{T}_h} \big(\operatorname{curl}\mathbf{E}_h, \phi_h\big)_K + \sum_{F\in\mathcal{F}_h^{\mathrm{int}}} \big(n_F \times [\![\mathbf{E}_h]\!]_F, \{\!\{\phi_h\}\!\}_F^{\mu c}\big)_F \\ &- \sum_{F\in\mathcal{F}_h^{\mathrm{bnd}}} \big(n_F \times \mathbf{E}_h, \phi_h\big)_F\ ,\end{aligned} \tag{2.21b}$$

respectively. The dG discretization of the Maxwell operator then reads

$$\boldsymbol{\mathcal{C}} = \begin{pmatrix} 0 & -\boldsymbol{\mathcal{C}}_\mathbf{E} \\ \boldsymbol{\mathcal{C}}_\mathbf{H} & 0 \end{pmatrix}. \tag{2.21c}$$

By (2.21a) and (2.21b) $\boldsymbol{\mathcal{C}}_\mathbf{H}$ and $\boldsymbol{\mathcal{C}}_\mathbf{E}$ are also well-defined on $D(\mathcal{C}_\mathbf{H}) \cap H^1(\mathcal{T}_h)^3$ and $D(\mathcal{C}_\mathbf{E}) \cap H^1(\mathcal{T}_h)^3$, respectively. Since functions in these spaces have vanishing tangential jumps,

$$n_F \times [\![\mathbf{U}]\!]_F = 0, \qquad \mathbf{U} \in D(\mathcal{C}_\mathbf{U}) \cap H^1(\mathcal{T}_h)^3, \qquad \mathbf{U} \in \{\mathbf{H}, \mathbf{E}\}, \tag{2.22}$$

the following consistency property holds true

$$\begin{aligned} \boldsymbol{\mathcal{C}}_{\mathbf{H}}\mathbf{H} &= \pi_h \mathcal{C}_{\mathbf{H}}\mathbf{H}, \qquad \mathbf{H} \in D(\mathcal{C}_{\mathbf{H}}) \cap H^1(\mathcal{T}_h)^3, \\ \boldsymbol{\mathcal{C}}_{\mathbf{E}}\mathbf{E} &= \pi_h \mathcal{C}_{\mathbf{E}}\mathbf{E}, \qquad \mathbf{E} \in D(\mathcal{C}_{\mathbf{E}}) \cap H^1(\mathcal{T}_h)^3. \end{aligned} \tag{2.23}$$

The following lemma is essential for our paper. It states that the discrete curl-operators preserve the adjointness property (2.11) of the continuous curl-operators.

LEMMA 2.2. *Given $\mathbf{H}_h, \mathbf{E}_h \in V_h$ there holds*

$$\left(\boldsymbol{\mathcal{C}}_{\mathbf{H}}\mathbf{H}_h, \mathbf{E}_h\right)_{\varepsilon} = \left(\mathbf{H}_h, \boldsymbol{\mathcal{C}}_{\mathbf{E}}\mathbf{E}_h\right)_{\mu}. \tag{2.24}$$

After space discretization we obtain the semidiscrete problem

$$\begin{aligned} \partial_t \mathbf{H}_h(t) &= -\boldsymbol{\mathcal{C}}_{\mathbf{E}}\mathbf{E}_h(t), \\ \partial_t \mathbf{E}_h(t) &= \boldsymbol{\mathcal{C}}_{\mathbf{H}}\mathbf{H}_h(t) - \mathbf{J}_h(t), \\ \mathbf{H}_h(0) &= \pi_h \mathbf{H}^0, \quad \mathbf{E}_h(0) = \pi_h \mathbf{E}^0, \\ \mathbf{J}_h(t) &= \pi_h(\varepsilon^{-1}\mathbf{J}). \end{aligned} \tag{2.25}$$

2.4. Splitting of discretized operators. We are interested in the situation where the mesh is split into a coarse and a fine part

$$\mathcal{T}_h = \mathcal{T}_{h,c} \,\dot{\cup}\, \mathcal{T}_{h,f}, \tag{2.26}$$

with the number of fine elements being small compared to the number of coarse ones:

$$0 < \operatorname{card}(\mathcal{T}_{h,f}) \ll \operatorname{card}(\mathcal{T}_{h,c}).$$

In order to obtain a scheme with a CFL condition independent of the fine part $\mathcal{T}_{h,f}$ it is necessary to treat the fine elements *and* their neighbors implicitly. The remaining elements can be treated explicitly. This motivates the following definition.

DEFINITION 2.3 (Mesh partitioning). *We partition the mesh into an implicitly and an explicitly treated part defined by*

$$\begin{aligned} \mathcal{T}_{h,i} &= \{K \in \mathcal{T}_h \mid \exists K_f \in \mathcal{T}_{h,f} \ : \ \operatorname{vol}_{d-1}(\partial K \cap \partial K_f) \neq 0\}, \\ \mathcal{T}_{h,e} &= \mathcal{T}_h \setminus \mathcal{T}_{h,i}, \end{aligned} \tag{2.27a}$$

respectively. Furthermore, we denote the set of implicitly treated elements which share a face with at least one explicitly treated element by

$$\mathcal{T}_{h,ci} = \{K_i \in \mathcal{T}_{h,i} \mid \exists K_e \in \mathcal{T}_{h,e} \ : \ \operatorname{vol}_{d-1}(\partial K_e \cap \partial K_i) \neq 0\}. \tag{2.27b}$$

Note that the explicitly treated set only contains coarse elements. In contrast, the implicitly treated set does not only contain fine elements but also their coarse neighbors. Furthermore, all elements in $\mathcal{T}_{h,ci}$ are coarse although they are treated implicitly:

$$\mathcal{T}_{h,e} \subset \mathcal{T}_{h,c}, \qquad \mathcal{T}_{h,f} \subset \mathcal{T}_{h,i}, \qquad \mathcal{T}_{h,i} \cap \mathcal{T}_{h,c} \neq \emptyset, \qquad \mathcal{T}_{h,ci} \subset \mathcal{T}_{h,c} \cap \mathcal{T}_{h,i}.$$

REMARK 2.4. *Although we do not consider conforming finite elements in this paper we point out that for this case the partitioning* (2.27a) *of the mesh $\mathcal{T}_h$ has to* *be adapted. Indeed, since in conforming finite element methods the coupling of the elements is done via the nodes (and not via the faces as in dG methods), one has to use the splitting*

$$\mathcal{T}_{h,i}^{\mathrm{FE}} = \{K \in \mathcal{T}_h \mid \exists K_f \in \mathcal{T}_{h,f} \ : \ \partial K \cap \partial K_f \neq \emptyset\},$$
$$\mathcal{T}_{h,e}^{\mathrm{FE}} = \mathcal{T}_h \setminus \mathcal{T}_{h,i}.$$

Note that by this definition the implicit set for finite element methods is a proper superset of the implicit set in dG methods, $\mathcal{T}_{h,i} \subsetneq \mathcal{T}_{h,i}^{\mathrm{FE}}$.

DEFINITION 2.5 (Face partitioning). *The set of interior faces is partitioned into*

$$\mathcal{F}_h^{\mathrm{int}} = \mathcal{F}_{h,i}^{\mathrm{int}} \,\dot\cup\, \mathcal{F}_{h,e}^{\mathrm{int}} \,\dot\cup\, \mathcal{F}_{h,ci}^{\mathrm{int}}, \tag{2.28}$$

where $\mathcal{F}_{h,i}^{\mathrm{int}}$ contains the faces between implicitly treated elements, $\mathcal{F}_{h,e}^{\mathrm{int}}$ the faces between explicitly treated elements and $\mathcal{F}_{h,ci}^{\mathrm{int}}$ the faces bordering an explicitly and an implicitly treated element. Furthermore, we write

$$\mathcal{F}_{h,c}^{\mathrm{int}} = \mathcal{F}_{h,e}^{\mathrm{int}} \cup \mathcal{F}_{h,ci}^{\mathrm{int}}. \tag{2.29}$$

It is important to observe that the set $\mathcal{F}_{h,c}^{\mathrm{int}}$ only contains faces bordering two coarse elements. We use the convention that for a face $F \in \mathcal{F}_{h,ci}^{\mathrm{int}}$ the normal n_F is directed from the implicit element K_i towards the explicit element K_e.

As in [4, Definition 1.38] we require the following regularity of the mesh $\mathcal{T}_h$.

ASSUMPTION 2.6. *We assume that the mesh $\mathcal{T}_h$ is shape regular, which means that there exist constants $\rho, \rho_c > 0$ independent of h such that*

$$\frac{h_K}{r_K} \leq \rho, \quad K \in \mathcal{T}_h, \qquad\qquad \frac{h_K}{r_K} \leq \rho_c, \quad K \in \mathcal{T}_{h,c},$$

where r_K denotes the radius of the largest ball inscribed in K.

Clearly, we have $\rho \geq \rho_c$ and for locally refined meshes we might have $\rho \gg \rho_c$. Assumption 2.6 implies

$$\rho^{-1} \max(h_K, h_{K_F}) \leq \frac{h_K + h_{K_F}}{2} \leq \rho \min(h_K, h_{K_F}), \qquad K, K_F \in \mathcal{T}_h, \tag{2.30a}$$

$$\rho_c^{-1} \max(h_K, h_{K_F}) \leq \frac{h_K + h_{K_F}}{2} \leq \rho_c \min(h_K, h_{K_F}), \qquad K, K_F \in \mathcal{T}_{h,c}, \tag{2.30b}$$

see, e.g., [4, Lemma 1.43]. Furthermore, the inverse inequality [4, Lemma 1.44] yields

$$\| \operatorname{curl} \mathbf{U}_h \|_K \leq C_{\mathrm{inv}} h_K^{-1} \| \mathbf{U}_h \|_K, \qquad K \in \mathcal{T}_h, \mathbf{U}_h \in V_h, \tag{2.31}$$

and the discrete trace inequality [4, Lemma 1.46] gives

$$\| \mathbf{U}_h \|_F \leq C_{\mathrm{tr}} h_K^{-1/2} \| \mathbf{U}_h \|_K, \qquad F \in \mathcal{F}_h, \mathbf{U}_h \in V_h. \tag{2.32}$$

The same bounds hold for K_F. The constants C_{inv} and C_{tr} depend on ρ, the polynomial degree k and the dimension d. On the coarse mesh $\mathcal{T}_{h,c}$ these inequalities hold true with dependency on ρ_c and k, d. We denote the corresponding constants by $C_{\mathrm{inv},c}$ and $C_{\mathrm{tr},c}$.

Let χ_i and χ_e denote the indicator functions on $\mathcal{T}_{h,i}$ and $\mathcal{T}_{h,e}$, respectively.

Definition 2.7. *We define the split discrete curl-operators as*

$$\boldsymbol{\mathcal{C}}_{\mathbf{H}}^b = \boldsymbol{\mathcal{C}}_{\mathbf{H}} \circ \chi_b, \qquad \boldsymbol{\mathcal{C}}_{\mathbf{E}}^b = \chi_b \circ \boldsymbol{\mathcal{C}}_{\mathbf{E}}, \qquad b \in \{i, e\}. \tag{2.33}$$

These are well-defined operators from $V_h + (D(\mathcal{C}_{\mathbf{H}}) \cap H^1(\mathcal{T}_h)^3)$ and $V_h + (D(\mathcal{C}_{\mathbf{E}}) \cap H^1(\mathcal{T}_h)^3)$ to V_h, respectively, which satisfy

$$\boldsymbol{\mathcal{C}}_{\mathbf{H}} = \boldsymbol{\mathcal{C}}_{\mathbf{H}}^i + \boldsymbol{\mathcal{C}}_{\mathbf{H}}^e, \qquad \boldsymbol{\mathcal{C}}_{\mathbf{E}} = \boldsymbol{\mathcal{C}}_{\mathbf{E}}^i + \boldsymbol{\mathcal{C}}_{\mathbf{E}}^e, \tag{2.34a}$$

and

$$\boldsymbol{\mathcal{C}}_{\mathbf{H}}^e \boldsymbol{\mathcal{C}}_{\mathbf{E}} = \boldsymbol{\mathcal{C}}_{\mathbf{H}}^e \boldsymbol{\mathcal{C}}_{\mathbf{E}}^e. \tag{2.34b}$$

It is easy to show that by (2.33) the split operators preserve the adjointness properties (2.11) and (2.24) from the continuous and the discretized curl-operators, respectively, i.e.,

$$\left(\boldsymbol{\mathcal{C}}_{\mathbf{H}}^b \mathbf{H}_h, \mathbf{E}_h\right)_\varepsilon = \left(\mathbf{H}_h, \boldsymbol{\mathcal{C}}_{\mathbf{E}}^b \mathbf{E}_h\right)_\mu, \qquad \mathbf{H}_h, \mathbf{E}_h \in V_h, \qquad b \in \{i, e\}. \tag{2.34c}$$

Let

$$c_{\infty,c} = \max_{K \in \mathcal{T}_{h,c}} c_K, \qquad c_\infty = \max_{K \in \mathcal{T}_h} c_K$$

be the maximum speed of light in the coarse grid and in the whole grid, respectively. A crucial observation is that the split curl-operators corresponding to the explicitly treated elements are bounded independently of the fine mesh. More precisely, $\boldsymbol{\mathcal{C}}_{\mathbf{H}}^e$ can be bounded w.r.t. the set $\mathcal{T}_{h,e} \subset \mathcal{T}_{h,c}$ and $\boldsymbol{\mathcal{C}}_{\mathbf{E}}^e$ w.r.t. $\mathcal{T}_{h,e} \cup \mathcal{T}_{h,ci} \subset \mathcal{T}_{h,c}$. However, the difference between these sets is negligible. Hence we omit it in the following and give the bounds involving the whole set $\mathcal{T}_{h,c}$ of coarse elements.

Theorem 2.8. *For $\mathbf{H}_h, \mathbf{E}_h \in V_h$ there holds*

$$\|\boldsymbol{\mathcal{C}}_{\mathbf{H}}^e \mathbf{H}_h\|_\varepsilon \leq C_{\mathrm{bnd},c} c_{\infty,c} \left(\sum_{K \in \mathcal{T}_{h,c}} h_K^{-2} \|\mathbf{H}_h\|_{\mu,K}^2 \right)^{1/2}, \tag{2.35a}$$

and

$$\|\boldsymbol{\mathcal{C}}_{\mathbf{E}}^e \mathbf{E}_h\|_\mu \leq C_{\mathrm{bnd},c} c_{\infty,c} \left(\sum_{K \in \mathcal{T}_{h,c}} h_K^{-2} \|\mathbf{E}_h\|_{\varepsilon,K}^2 \right)^{1/2}, \tag{2.35b}$$

where

$$C_{\mathrm{bnd},c} = C_{\mathrm{inv},c} + 2C_{\mathrm{tr},c}^2 N_\partial \rho_c. \tag{2.35c}$$

So far, the split operators inherited the properties of the full operators. By the construction of the $\boldsymbol{\mathcal{C}}_{\mathbf{E}}^b$ operators this also holds true for the consistency property (2.23), i.e.,

$$\boldsymbol{\mathcal{C}}_{\mathbf{E}}^b \mathbf{E} = \chi_b(\pi_h \mathcal{C}_{\mathbf{E}} \mathbf{E}), \qquad \mathbf{E} \in D(\mathcal{C}_{\mathbf{E}}) \cap H^1(\mathcal{T}_h)^3, \qquad b \in \{i, e\}. \tag{2.36}$$

In particular, we have

$$\|\boldsymbol{\mathcal{C}}_{\mathbf{E}}^b \mathbf{E}\|_\mu \leq \mu_0^{-1/2} \|\operatorname{curl} \mathbf{E}\|_{\mathcal{T}_{h,b}}, \qquad \mathbf{E} \in D(\mathcal{C}_{\mathbf{E}}) \cap H^1(\mathcal{T}_h)^3, \qquad b \in \{i, e\}. \tag{2.37}$$

Unfortunately this is not true for the $\mathcal{C}_{\mathbf{H}}^b$ operators. Thus we cannot obtain a uniform bound like (2.37) but only one involving $h_K^{-1/2}$.

LEMMA 2.9. *For* $\mathbf{H} \in D(\mathcal{C}_{\mathbf{H}}) \cap H^1(\mathcal{T}_h)^3$ *there holds*

$$\|\mathcal{C}_{\mathbf{H}}^e \mathbf{H}\|_\varepsilon \le \varepsilon_0^{-1/2} \|\operatorname{curl} \mathbf{H}\|_{\mathcal{T}_{h,e}} + C'_{\mathrm{bnd,c}} \varepsilon_0^{-1/2} \left(\sum_{F \in \mathcal{F}_{h,ci}^{\mathrm{int}}} h_{K_e}^{-1} \|\mathbf{H}\|_{1,K_e}^2 \right)^{1/2}, \tag{2.38}$$

where K_e *denotes the explicit element corresponding to the face* $F \in \mathcal{F}_{h,ci}^{\mathrm{int}}$ *and* $C'_{\mathrm{bnd,c}} = C_{\mathrm{ctr,c}} C_{\mathrm{tr,c}} N_\partial^{1/2} \rho_c$. *The constant* $C_{\mathrm{ctr,c}}$ *is given in* (A.12).

3. Locally implicit time integration. Next, we consider the time integration of (2.25).

3.1. Time integration methods. For the time integration of the semidiscrete Maxwell's equations (2.25), Verwer [15] proposed a blend of two well-known schemes, namely the explicit Verlet (or leap-frog) method

$$\begin{aligned} \mathbf{H}_h^{n+1/2} - \mathbf{H}_h^n &= -\frac{\tau}{2} \mathcal{C}_{\mathbf{E}} \mathbf{E}_h^n, \\ \mathbf{E}_h^{n+1} - \mathbf{E}_h^n &= \tau \mathcal{C}_{\mathbf{H}} \mathbf{H}_h^{n+1/2} - \frac{\tau}{2} (\mathbf{J}_h^{n+1} + \mathbf{J}_h^n), \\ \mathbf{H}_h^{n+1} - \mathbf{H}_h^{n+1/2} &= -\frac{\tau}{2} \mathcal{C}_{\mathbf{E}} \mathbf{E}_h^{n+1}, \end{aligned} \tag{3.1}$$

and the implicit Crank–Nicolson method which we write as

$$\begin{aligned} \mathbf{H}_h^{n+1/2} - \mathbf{H}_h^n &= -\frac{\tau}{2} \mathcal{C}_{\mathbf{E}} \mathbf{E}_h^n, \\ \mathbf{E}_h^{n+1} - \mathbf{E}_h^n &= \frac{\tau}{2} \mathcal{C}_{\mathbf{H}} (\mathbf{H}_h^{n+1} + \mathbf{H}_h^n) - \frac{\tau}{2} (\mathbf{J}_h^{n+1} + \mathbf{J}_h^n), \\ \mathbf{H}_h^{n+1} - \mathbf{H}_h^{n+1/2} &= -\frac{\tau}{2} \mathcal{C}_{\mathbf{E}} \mathbf{E}_h^{n+1}. \end{aligned} \tag{3.2}$$

Here $\tau > 0$ denotes the time step size and $\mathbf{H}_h^{n+1} \approx \mathbf{H}_h(t_{n+1}) \approx \mathbf{H}(t_{n+1})$, $\mathbf{E}_h^{n+1} \approx \mathbf{E}_h(t_{n+1}) \approx \mathbf{E}(t_{n+1})$ denote the fully discrete approximations at time $t_{n+1} = (n+1)\tau$. It is well-known that both schemes are of classical order two. While the Crank–Nicolson scheme is unconditionally stable, the Verlet method is stable under the CFL condition [15, Sec. 2]

$$\tau < \frac{2}{\sqrt{\|\mathcal{C}_{\mathbf{H}} \mathcal{C}_{\mathbf{E}}\|_\varepsilon}}.$$

By using $\mathcal{T}_{h,e} = \mathcal{T}_h$ in Theorem 2.8 we conclude

$$\|\mathcal{C}_{\mathbf{H}} \mathbf{H}_h\|_\varepsilon \le C_{\mathrm{bnd}} c_\infty \left(\sum_{K \in \mathcal{T}_h} h_K^{-2} \|\mathbf{H}_h\|_{\mu,K}^2 \right)^{1/2}, \qquad \mathbf{H}_h \in V_h, \tag{3.3a}$$

and

$$\|\mathcal{C}_{\mathbf{E}} \mathbf{E}_h\|_\mu \le C_{\mathrm{bnd}} c_\infty \left(\sum_{K \in \mathcal{T}_h} h_K^{-2} \|\mathbf{E}_h\|_{\varepsilon,K}^2 \right)^{1/2}, \qquad \mathbf{E}_h \in V_h, \tag{3.3b}$$

where $C_{\mathrm{bnd}} = C_{\mathrm{inv}} + 2C_{\mathrm{tr}}^2 N_\partial \rho$. Hence, the CFL condition for the Verlet method is

$$\tau < \frac{2}{C_{\mathrm{bnd}} c_\infty} \min_{K \in \mathcal{T}_h} h_K. \tag{3.4}$$

The Crank–Nicolson method preserves the electromagnetic energy $\mathcal{E}(\mathbf{H}_h, \mathbf{E}_h)$ defined in (2.12) whereas the Verlet scheme preserves the perturbed energy

$$\mathcal{E}(\mathbf{H}_h, \mathbf{E}_h) - \frac{\tau^2}{8} \|\boldsymbol{\mathcal{C}}_{\mathbf{E}} \mathbf{E}_h\|_\mu^2, \tag{3.5}$$

see [15, Sec. 2], for instance.

Verwer's idea was to use the explicit scheme on the "coarse" part of the grid and the implicit scheme on the "fine" part of the grid.

However, his splitting was solely based on the ode formulation and hence it was not clear which elements have to be treated explicitly and which have to be treated implicitly in order to guarantee stability and error bounds independent of the fine part of the mesh. We adapt Verwer's idea by using the split discrete curl-operators defined in (2.33). This yields the following scheme:

$$\mathbf{H}_h^{n+1/2} - \mathbf{H}_h^n = -\frac{\tau}{2} \boldsymbol{\mathcal{C}}_{\mathbf{E}} \mathbf{E}_h^n, \tag{3.6a}$$

$$\mathbf{E}_h^{n+1} - \mathbf{E}_h^n = \tau \boldsymbol{\mathcal{C}}_{\mathbf{H}}^e \mathbf{H}_h^{n+1/2} + \frac{\tau}{2} \boldsymbol{\mathcal{C}}_{\mathbf{H}}^i (\mathbf{H}_h^{n+1} + \mathbf{H}_h^n) - \frac{\tau}{2} (\mathbf{J}_h^{n+1} + \mathbf{J}_h^n), \tag{3.6b}$$

$$\mathbf{H}_h^{n+1} - \mathbf{H}_h^{n+1/2} = -\frac{\tau}{2} \boldsymbol{\mathcal{C}}_{\mathbf{E}} \mathbf{E}_h^{n+1}. \tag{3.6c}$$

3.2. Analysis of the locally implicit method. We start our analysis by writing the locally implicit scheme (3.6) in a compact form.

LEMMA 3.1. *For* $\mathbf{u}_h^n = (\mathbf{H}_h^n, \mathbf{E}_h^n)$ *the recursion* (3.6) *can be written as*

$$\boldsymbol{\mathcal{R}}_L \mathbf{u}_h^{n+1} = \boldsymbol{\mathcal{R}}_R \mathbf{u}_h^n + \mathbf{j}_h^n, \qquad \mathbf{j}_h^n = -\frac{\tau}{2} \begin{pmatrix} 0 \\ \mathbf{J}_h^{n+1} + \mathbf{J}_h^n \end{pmatrix}, \tag{3.7a}$$

with operators $\boldsymbol{\mathcal{R}}_L$, $\boldsymbol{\mathcal{R}}_R$ *defined by*

$$\boldsymbol{\mathcal{R}}_L = \begin{pmatrix} \mathcal{I} & \frac{\tau}{2} \boldsymbol{\mathcal{C}}_{\mathbf{E}} \\ -\frac{\tau}{2} \boldsymbol{\mathcal{C}}_{\mathbf{H}} & \mathcal{I} - \frac{\tau^2}{4} \boldsymbol{\mathcal{C}}_{\mathbf{H}}^e \boldsymbol{\mathcal{C}}_{\mathbf{E}}^e \end{pmatrix}, \qquad \boldsymbol{\mathcal{R}}_R = \begin{pmatrix} \mathcal{I} & -\frac{\tau}{2} \boldsymbol{\mathcal{C}}_{\mathbf{E}} \\ \frac{\tau}{2} \boldsymbol{\mathcal{C}}_{\mathbf{H}} & \mathcal{I} - \frac{\tau^2}{4} \boldsymbol{\mathcal{C}}_{\mathbf{H}}^e \boldsymbol{\mathcal{C}}_{\mathbf{E}}^e \end{pmatrix}. \tag{3.7b}$$

Proof. The first component of (3.7a) is obtained by adding (3.6a) and (3.6c). For the second component we subtract (3.6c) from (3.6a):

$$\mathbf{H}_h^{n+1/2} = \frac{1}{2} (\mathbf{H}_h^{n+1} + \mathbf{H}_h^n) + \frac{\tau}{4} \boldsymbol{\mathcal{C}}_{\mathbf{E}} (\mathbf{E}_h^{n+1} - \mathbf{E}_h^n).$$

Inserting this into (3.6b) we infer

$$\mathbf{E}_h^{n+1} - \mathbf{E}_h^n = \frac{\tau}{2} \boldsymbol{\mathcal{C}}_{\mathbf{H}} (\mathbf{H}_h^{n+1} + \mathbf{H}_h^n) + \frac{\tau^2}{4} \boldsymbol{\mathcal{C}}_{\mathbf{H}}^e \boldsymbol{\mathcal{C}}_{\mathbf{E}}^e (\mathbf{E}_h^{n+1} - \mathbf{E}_h^n) - \frac{\tau}{2} (\mathbf{J}_h^{n+1} + \mathbf{J}_h^n), \tag{3.8}$$

by using $\boldsymbol{\mathcal{C}}_{\mathbf{H}}^e + \boldsymbol{\mathcal{C}}_{\mathbf{H}}^i = \boldsymbol{\mathcal{C}}_{\mathbf{H}}$ and $\boldsymbol{\mathcal{C}}_{\mathbf{H}}^e \boldsymbol{\mathcal{C}}_{\mathbf{E}} = \boldsymbol{\mathcal{C}}_{\mathbf{H}}^e \boldsymbol{\mathcal{C}}_{\mathbf{E}}^e$, see (2.34a) and (2.34b). ∎

The next lemma gives two fundamental properties of the operators $\boldsymbol{\mathcal{R}}_L$ and $\boldsymbol{\mathcal{R}}_R$.

LEMMA 3.2. *For $\mathbf{u}_h, \widehat{\mathbf{u}}_h \in V_h \times V_h$ it holds*

$$\big(\boldsymbol{\mathcal{R}}_L \mathbf{u}_h, \widehat{\mathbf{u}}_h\big)_{\mu\times\varepsilon} = \big(\mathbf{u}_h, \boldsymbol{\mathcal{R}}_R \widehat{\mathbf{u}}_h\big)_{\mu\times\varepsilon}. \tag{3.9}$$

Furthermore, for $\mathbf{u}_h = (\mathbf{H}_h, \mathbf{E}_h) \in V_h \times V_h$ we have

$$\big(\boldsymbol{\mathcal{R}}_L \mathbf{u}_h, \mathbf{u}_h\big)_{\mu\times\varepsilon} = \|\mathbf{u}_h\|^2_{\mu\times\varepsilon} - \frac{\tau^2}{4}\|\boldsymbol{\mathcal{C}}^e_{\mathbf{E}}\mathbf{E}_h\|^2_{\mu}. \tag{3.10}$$

Proof. These results emerge directly from the adjointness properties (2.24) and (2.34c) of the discrete and the split discrete curl-operators, respectively. ∎

4. Stability. Next we prove the well-posedness and the stability of the locally implicit scheme (3.6) under a CFL condition that solely depends on the size of mesh elements in the coarse mesh $\mathcal{T}_{h,c}$.

Let $0 < \delta < 1$ be an arbitrary but fixed parameter. Then the CFL condition reads

$$\tau \leq \frac{2\sqrt{\delta}}{C_{\mathrm{bnd},c}c_{\infty,c}} \min_{K\in\mathcal{T}_{h,c}} h_K, \tag{4.1}$$

where $C_{\mathrm{bnd},c}$ was defined in (2.35c). The next lemma states that if (4.1) is satisfied, then the approximations obtained from (3.6) are well defined (independent of the fine part of the spatial grid). Furthermore, it proves that $\big(\boldsymbol{\mathcal{R}}_L\cdot,\cdot\big)_{\mu\times\varepsilon}$ defines a norm which is equivalent to the weighted L^2-norm $\|\cdot\|_{\mu\times\varepsilon}$. This will be crucial for the proof of stability.

LEMMA 4.1. *Let $\mathbf{u}_h \in V_h \times V_h$ and assume that the CFL condition* (4.1) *is satisfied. Then, we have*

$$(1-\delta)\|\mathbf{u}_h\|^2_{\mu\times\varepsilon} \leq \big(\boldsymbol{\mathcal{R}}_L \mathbf{u}_h, \mathbf{u}_h\big)_{\mu\times\varepsilon} \leq \|\mathbf{u}_h\|^2_{\mu\times\varepsilon}. \tag{4.2}$$

In particular, $\boldsymbol{\mathcal{R}}_L$ is invertible with bound

$$\|\boldsymbol{\mathcal{R}}_L^{-1}\mathbf{u}_h\|_{\mu\times\varepsilon} \leq C_{\mathrm{stb}}\|\mathbf{u}_h\|_{\mu\times\varepsilon}, \qquad C_{\mathrm{stb}} = (1-\delta)^{-1}. \tag{4.3}$$

Proof. The upper bound in (4.2) follows immediatly from (3.10). For the lower bound we show that the negative term in (3.10) is uniformly bounded away from zero. In fact, we use Theorem 2.8 and the CFL condition (4.1) to infer

$$\frac{\tau^2}{4}\|\boldsymbol{\mathcal{C}}^e_{\mathbf{E}}\mathbf{E}_h\|^2_{\mu} \leq \frac{\tau^2}{4}C^2_{\mathrm{bnd},c}c^2_{\infty,c}\sum_{K\in\mathcal{T}_{h,c}} h_K^{-2}\|\mathbf{E}_h\|^2_{\varepsilon,K} \leq \delta\|\mathbf{E}_h\|^2_{\varepsilon,\mathcal{T}_{h,c}} \leq \delta\|\mathbf{u}_h\|^2_{\mu\times\varepsilon}. \tag{4.4}$$

Thus, we conclude

$$\big(\boldsymbol{\mathcal{R}}_L \mathbf{u}_h, \mathbf{u}_h\big)_{\mu\times\varepsilon} = \|\mathbf{u}_h\|^2_{\mu\times\varepsilon} - \frac{\tau^2}{4}\|\boldsymbol{\mathcal{C}}^e_{\mathbf{E}}\mathbf{E}_h\|^2_{\mu} \geq (1-\delta)\|\mathbf{u}_h\|^2_{\mu\times\varepsilon}, \tag{4.5}$$

which is the desired lower bound in (4.2). Clearly, this implies that $\boldsymbol{\mathcal{R}}_L$ is an isomorphism on $V_h \times V_h$ satisfying (4.3). ∎

As a consequence, if we assume that the CFL condition (4.1) is satisfied, we can write (3.7a) as

$$\mathbf{u}_h^{n+1} = \boldsymbol{\mathcal{R}}\mathbf{u}_h^n + \boldsymbol{\mathcal{R}}_L^{-1}\mathbf{j}_h^n, \qquad \text{where} \qquad \boldsymbol{\mathcal{R}} = \boldsymbol{\mathcal{R}}_L^{-1}\boldsymbol{\mathcal{R}}_R. \tag{4.6}$$

Solving the recursion yields

$$\mathbf{u}_h^{n+1} = \boldsymbol{\mathcal{R}}^{n+1}\mathbf{u}_h^0 + \sum_{m=0}^{n} \boldsymbol{\mathcal{R}}^{n-m}\boldsymbol{\mathcal{R}}_L^{-1}\mathbf{j}_h^m. \tag{4.7}$$

The last step towards proving stability for (3.6) is to bound powers of the operator $\boldsymbol{\mathcal{R}}$. Again, it is crucial to observe that this bound is independent of the fine part of the spatial mesh.

LEMMA 4.2. *Let $\mathbf{u}_h = (\mathbf{H}_h, \mathbf{E}_h) \in V_h \times V_h$. Then, under the CFL condition* (4.1) *the following bound is satisfied for all $m \in \mathbb{N}$*

$$\|\boldsymbol{\mathcal{R}}^m \mathbf{u}_h\|_{\mu\times\varepsilon}^2 \le C_{\mathrm{stb}}\Big(\|\mathbf{u}_h\|_{\mu\times\varepsilon}^2 - \frac{\tau^2}{4}\|\boldsymbol{\mathcal{C}}_{\mathbf{E}}^e \mathbf{E}_h\|_\mu^2\Big) \le C_{\mathrm{stb}}\|\mathbf{u}_h\|_{\mu\times\varepsilon}^2. \tag{4.8}$$

Proof. By (4.2) it is sufficient to consider $\big(\boldsymbol{\mathcal{R}}_L\boldsymbol{\mathcal{R}}^m\mathbf{u}_h, \boldsymbol{\mathcal{R}}^m\mathbf{u}_h\big)$. Using (3.9) we infer

$$\begin{aligned}
\big(\boldsymbol{\mathcal{R}}_L\boldsymbol{\mathcal{R}}^m\mathbf{u}_h, \boldsymbol{\mathcal{R}}^m\mathbf{u}_h\big)_{\mu\times\varepsilon} &= \big(\boldsymbol{\mathcal{R}}_R\boldsymbol{\mathcal{R}}^{m-1}\mathbf{u}_h, \boldsymbol{\mathcal{R}}^m\mathbf{u}_h\big)_{\mu\times\varepsilon} \\
&= \big(\boldsymbol{\mathcal{R}}^{m-1}\mathbf{u}_h, \boldsymbol{\mathcal{R}}_L\boldsymbol{\mathcal{R}}^m\mathbf{u}_h\big)_{\mu\times\varepsilon} \\
&= \big(\boldsymbol{\mathcal{R}}^{m-1}\mathbf{u}_h, \boldsymbol{\mathcal{R}}_R\boldsymbol{\mathcal{R}}^{m-1}\mathbf{u}_h\big)_{\mu\times\varepsilon} \\
&= \big(\boldsymbol{\mathcal{R}}_L\boldsymbol{\mathcal{R}}^{m-1}\mathbf{u}_h, \boldsymbol{\mathcal{R}}^{m-1}\mathbf{u}_h\big)_{\mu\times\varepsilon} \\
&= \dots \\
&= \big(\boldsymbol{\mathcal{R}}_L\mathbf{u}_h, \mathbf{u}_h\big)_{\mu\times\varepsilon}.
\end{aligned}$$

(4.2) and (3.10) then show

$$(1-\delta)\|\boldsymbol{\mathcal{R}}^m\mathbf{u}_h\|_{\mu\times\varepsilon}^2 \le \big(\boldsymbol{\mathcal{R}}_L\boldsymbol{\mathcal{R}}^m\mathbf{u}_h, \boldsymbol{\mathcal{R}}^m\mathbf{u}_h\big)_{\mu\times\varepsilon} = \|\mathbf{u}_h\|_{\mu\times\varepsilon}^2 - \frac{\tau^2}{4}\|\boldsymbol{\mathcal{C}}_{\mathbf{E}}^e\mathbf{E}_h\|_\mu^2,$$

$m = 1, 2, \dots$, which completes the proof. ∎

LEMMA 4.3. *For $\mathbf{J} \equiv 0$, the approximation $(\mathbf{H}_h^n, \mathbf{E}_h^n)$ obtained from the scheme* (3.6) *conserves the discrete energy*

$$\mathcal{E}_h(\mathbf{H}_h, \mathbf{E}_h) = \mathcal{E}(\mathbf{H}_h, \mathbf{E}_h) - \frac{\tau^2}{8}\|\boldsymbol{\mathcal{C}}_{\mathbf{E}}^e\mathbf{E}_h\|_\mu^2, \tag{4.9}$$

i.e., $\mathcal{E}_h(\mathbf{H}_h^n, \mathbf{E}_h^n) = \mathcal{E}_h(\mathbf{H}_h^0, \mathbf{E}_h^0)$*,* $n = 1, 2, \dots$*.*

Note that the energy which is conserved by the locally implicit method is equal to the energy of the Verlet method (3.5) but the full operator $\boldsymbol{\mathcal{C}}_{\mathbf{E}}$ is replaced by its explicit part $\boldsymbol{\mathcal{C}}_{\mathbf{E}}^e$.

Proof. For $\mathbf{J} \equiv 0$ we have $\mathbf{u}_h^n = \boldsymbol{\mathcal{R}}^n\mathbf{u}_h^0$, see (4.7). Thus the proof of the previous lemma shows that

$$\big(\boldsymbol{\mathcal{R}}_L\mathbf{u}_h^n, \mathbf{u}_h^n\big)_{\mu\times\varepsilon} = \big(\boldsymbol{\mathcal{R}}_L\mathbf{u}_h^0, \mathbf{u}_h^0\big)_{\mu\times\varepsilon}. \tag{4.10}$$

The statement then follows from (3.10). ∎

Now, we have all ingredients to prove stability of the locally implicit method (3.6). In fact, this can be seen as a discrete analogon of the bound (2.13) of the exact solution.

THEOREM 4.4. *Let* $0 < \delta < 1$ *and assume that the CFL condition* (4.1) *is satisfied. Then, the approximation* $\mathbf{u}_h^n = (\mathbf{H}_h^n, \mathbf{E}_h^n)$ *obtained from* (3.6) *is bounded by*

$$\|\mathbf{u}_h^n\|_{\mu\times\varepsilon} \le C_{\mathrm{stb}}^{1/2}\|\mathbf{u}^0\|_{\mu\times\varepsilon} + C_{\mathrm{stb}}^{3/2}\tau\sum_{m=0}^{n-1}\frac{1}{2}\|\mathbf{J}^{m+1}+\mathbf{J}^m\| \tag{4.11}$$

for step sizes τ *such that* $n\tau \le T$.

Proof. From (4.7) and the triangle inequality we have

$$\begin{aligned}\|\mathbf{u}_h^n\|_{\mu\times\varepsilon} \le& \|\boldsymbol{\mathcal{R}}^n\mathbf{u}_h^0\|_{\mu\times\varepsilon} + \sum_{m=0}^{n-1}\|\boldsymbol{\mathcal{R}}^{n-m}\boldsymbol{\mathcal{R}}_L^{-1}\mathbf{j}_h^m\|_{\mu\times\varepsilon}\\ \le& C_{\mathrm{stb}}^{1/2}\|\mathbf{u}_h^0\|_{\mu\times\varepsilon} + C_{\mathrm{stb}}^{3/2}\sum_{m=0}^{n-1}\|\mathbf{j}_h^m\|_{\mu\times\varepsilon}.\end{aligned}$$

Here, the second inequality is obtained from (4.3) and (4.8). Inserting the definition of $\mathbf{u}_h^0$ and $\mathbf{j}_h^m$ and using the boundedness of the projection operator π_h yields the result. ∎

5. Error analysis. Let $\mathbf{u}^n = (\mathbf{H}^n, \mathbf{E}^n) = (\mathbf{H}(t_n), \mathbf{E}(t_n)) \in C^3\big(0, T; L^2(\Omega)^6\big)$ be the exact solution of (2.6) at time t_n and denote by $\mathbf{u}_h^n = (\mathbf{H}_h^n, \mathbf{E}_h^n) \approx \mathbf{u}^n$ the approximation obtained by the dG discretization and the locally implicit scheme (3.6). The full discretization error is given by

$$\mathbf{e}^n = \begin{pmatrix}\mathbf{e}_{\mathbf{H}}^n\\ \mathbf{e}_{\mathbf{E}}^n\end{pmatrix} = \begin{pmatrix}\mathbf{H}^n - \mathbf{H}_h^n\\ \mathbf{E}^n - \mathbf{E}_h^n\end{pmatrix}. \tag{5.1}$$

As usual, we split it into

$$\mathbf{e}^n = \mathbf{e}_\pi^n - \mathbf{e}_h^n = \begin{pmatrix}\mathbf{H}^n - \pi_h\mathbf{H}^n\\ \mathbf{E}^n - \pi_h\mathbf{E}^n\end{pmatrix} - \begin{pmatrix}\mathbf{H}_h^n - \pi_h\mathbf{H}^n\\ \mathbf{E}_h^n - \pi_h\mathbf{E}^n\end{pmatrix}. \tag{5.2}$$

By Assumption 2.6 the mesh $\mathcal{T}_h$ has optimal polynomial approximation properties [4, Lemma 1.62] in the sense of [4, Definition 1.55]. Thus, for the projection error $\mathbf{e}_\pi^n = (\mathbf{e}_{\pi,\mathbf{H}}^n, \mathbf{e}_{\pi,\mathbf{E}}^n)$ the following approximation results hold true [4, Lemmas 1.58, 1.59]: For $K \in \mathcal{T}_h$, $F \in \mathcal{F}_h$, and $\mathbf{H}, \mathbf{E} \in H^{k+1}(K)^3$ there are constants C_{app}, C'_{app} such that the projection errors satisfy

$$\|\mathbf{e}_{\pi,\mathbf{H}}\|_{\mu,K} \le C_{\mathrm{app}}h_K^{k+1}|\mathbf{H}|_{k+1,K}, \qquad \|\mathbf{e}_{\pi,\mathbf{E}}\|_{\varepsilon,K} \le C_{\mathrm{app}}h_K^{k+1}|\mathbf{E}|_{k+1,K}, \tag{5.3a}$$

$$\|\mathbf{e}_{\pi,\mathbf{H}}\|_{\mu,F} \le C'_{\mathrm{app}}h_K^{k+1/2}|\mathbf{H}|_{k+1,K}, \qquad \|\mathbf{e}_{\pi,\mathbf{E}}\|_{\varepsilon,F} \le C'_{\mathrm{app}}h_K^{k+1/2}|\mathbf{E}|_{k+1,K}, \tag{5.3b}$$

and

$$\|\operatorname{curl}\mathbf{e}_{\pi,\mathbf{H}}\|_{\mu,K} \le C_{\mathrm{app}}h_K^{k}|\mathbf{H}|_{k+1,K}, \qquad \|\operatorname{curl}\mathbf{e}_{\pi,\mathbf{E}}\|_{\varepsilon,K} \le C_{\mathrm{app}}h_K^{k}|\mathbf{E}|_{k+1,K}. \tag{5.3c}$$

The constants $C_{\mathrm{app}}, C'_{\mathrm{app}}$ depend on ρ but are independent of both the mesh element K and its size h_K. Let $\mathbf{H} \in D(\mathcal{C}_{\mathbf{H}}) \cap H^{k+1}(\mathcal{T}_h)^3$ and $\mathbf{E} \in D(\mathcal{C}_{\mathbf{E}}) \cap H^{k+1}(\mathcal{T}_h)^3$. Then, it holds

$$\|\boldsymbol{\mathcal{C}}_{\mathbf{H}}^e\mathbf{e}_{\pi,\mathbf{H}}\|_\varepsilon \le C_{\pi,c}\left(\sum_{K\in\mathcal{T}_{h,c}} h_K^{2k}|\mathbf{H}|_{k+1,K}^2\right)^{1/2}, \tag{5.4a}$$

$$\|\boldsymbol{\mathcal{C}}_{\mathbf{E}}^e\mathbf{e}_{\pi,\mathbf{E}}\|_\mu \le C_{\pi,c}\left(\sum_{K\in\mathcal{T}_{h,c}} h_K^{2k}|\mathbf{E}|_{k+1,K}^2\right)^{1/2}, \tag{5.4b}$$

and for $\mathbf{u} = (\mathbf{H}, \mathbf{E})$ we have

$$\|\boldsymbol{\mathcal{C}}\mathbf{e}_\pi\|_{\mu\times\varepsilon} \le C_\pi \Big(\sum_{K\in\mathcal{T}_h} h_K^{2k} |\mathbf{u}|_{k+1,K}^2 \Big)^{1/2}, \tag{5.5}$$

where $C_{\pi,c} = (C_{\mathrm{app}} + 2C'_{\mathrm{app}} C_{\mathrm{tr},c} N_\partial \rho_c) c_{\infty,c}$ and $C_\pi = (C_{\mathrm{app}} + 2C'_{\mathrm{app}} C_{\mathrm{tr}} N_\partial \rho) c_\infty$. The bounds (5.4) can be shown with a similar proof as for Theorem 2.8 with the following two changes: The inverse inequality in (A.2) is replaced by (5.3c) and the discrete trace inequality in (A.4) is replaced by (5.3b). The result (5.5) is obtained by using $\mathcal{T}_{h,e} = \mathcal{T}_h$.

5.1. Error recursion. In the next lemma we prove that the error $\mathbf{e}_h^n$ satisfies a perturbed version of the recursion (3.7a) of the approximation $\mathbf{u}_h^n$.

LEMMA 5.1. *Let the exact solution satisfy $\mathbf{u} \in C\big(0, T; H^{k+1}(\mathcal{T}_h)^6\big)$. Under the CFL condition (4.1) the error $\mathbf{e}_h^n$ defined in (5.2) satisfies*

$$\boldsymbol{\mathcal{R}}_L \mathbf{e}_h^{n+1} = \boldsymbol{\mathcal{R}}_R \mathbf{e}_h^n + \mathbf{d}^n \tag{5.6}$$

with defect $\mathbf{d}^n = \mathbf{d}_\pi^n + \mathbf{d}_h^n$ given by

$$\mathbf{d}_\pi^n = \frac{\tau}{2}\boldsymbol{\mathcal{C}}(\mathbf{e}_\pi^{n+1} + \mathbf{e}_\pi^n) - \frac{\tau^2}{4}\begin{pmatrix} 0 \\ \boldsymbol{\mathcal{C}}_{\mathbf{H}}^e \boldsymbol{\mathcal{C}}_{\mathbf{E}}^e \big(\mathbf{e}_{\pi,\mathbf{E}}^{n+1} - \mathbf{e}_{\pi,\mathbf{E}}^n\big)\end{pmatrix}, \tag{5.7a}$$

$$\mathbf{d}_h^n = \tau^2 \pi_h \delta^n - \frac{\tau^2}{4}\begin{pmatrix} 0 \\ \boldsymbol{\mathcal{C}}_{\mathbf{H}}^e \pi_h \Delta_{\mathbf{H}}^n \end{pmatrix}. \tag{5.7b}$$

The projection defect $\mathbf{d}_\pi^n$ is bounded by

$$\begin{aligned} \|\mathbf{d}_\pi^n\|_{\mu\times\varepsilon} \le & C_\pi \frac{\tau}{2}\Big(\sum_{K\in\mathcal{T}_h} h_K^{2k} |\mathbf{u}^{n+1} + \mathbf{u}^n|_{k+1,K}^2 \Big)^{1/2} \\ & + C_{\pi,c}\frac{\tau}{2}\Big(\sum_{K\in\mathcal{T}_{h,c}} h_K^{2k} |\mathbf{E}^{n+1} - \mathbf{E}^n|_{k+1,K}^2 \Big)^{1/2}. \end{aligned} \tag{5.8}$$

The quadrature defect $\delta^n = (\delta_{\mathbf{H}}^n, \delta_{\mathbf{E}}^n)$ is bounded by

$$\|\delta^n\|_{\mu\times\varepsilon} \le \frac{1}{8}\int_{t_n}^{t_{n+1}} \|\partial_t^3 \mathbf{u}(t)\|_{\mu\times\varepsilon}\, dt, \tag{5.9}$$

and the quadrature defect $\Delta_{\mathbf{H}}^n$ is given by

$$\Delta_{\mathbf{H}}^n = \int_{t_n}^{t_{n+1}} \partial_t^2 \mathbf{H}(t)\, dt. \tag{5.10}$$

Proof. The defects are obtained by inserting the projected exact solution into the numerical scheme (3.6). For the $\mathbf{H}$-component the scheme reads

$$\mathbf{H}_h^{n+1} - \mathbf{H}_h^n = -\frac{\tau}{2}\boldsymbol{\mathcal{C}}_{\mathbf{E}}\big(\mathbf{E}_h^{n+1} + \mathbf{E}_h^n\big). \tag{5.11}$$

The iteration for the $\mathbf{E}$-component is taken from (3.8). For $\mathbf{d}^n = (\mathbf{d}^n_{\mathbf{H}}, \mathbf{d}^n_{\mathbf{E}})$ this yields

$$
\begin{aligned}
\pi_h(\mathbf{H}^{n+1} - \mathbf{H}^n) &= -\frac{\tau}{2}\boldsymbol{\mathcal{C}}_{\mathbf{E}}\pi_h(\mathbf{E}^{n+1} + \mathbf{E}^n) - \mathbf{d}^n_{\mathbf{H}}, \\
\pi_h(\mathbf{E}^{n+1} - \mathbf{E}^n) &= \frac{\tau}{2}\boldsymbol{\mathcal{C}}_{\mathbf{H}}\pi_h(\mathbf{H}^{n+1} + \mathbf{H}^n) + \frac{\tau^2}{4}\boldsymbol{\mathcal{C}}^e_{\mathbf{H}}\boldsymbol{\mathcal{C}}^e_{\mathbf{E}}\pi_h(\mathbf{E}^{n+1} - \mathbf{E}^n) \\
&\quad - \frac{\tau}{2}(\mathbf{J}_h^{n+1} + \mathbf{J}_h^n) - \mathbf{d}^n_{\mathbf{E}}.
\end{aligned} \tag{5.12}
$$

The desired expressions for $\mathbf{d}^n$ are obtained via Taylor expansion of $(\mathbf{H}(t_{n+1/2}), \mathbf{E}(t_{n+1/2}))$ around t_n and t_{n+1}, respectively. This gives

$$
\begin{aligned}
\mathbf{H}^{n+1} - \mathbf{H}^n &= \frac{\tau}{2}(\partial_t\mathbf{H}^{n+1} + \partial_t\mathbf{H}^n) - \tau^2\delta^n_{\mathbf{H}}, \\
\mathbf{E}^{n+1} - \mathbf{E}^n &= \frac{\tau}{2}(\partial_t\mathbf{E}^{n+1} + \partial_t\mathbf{E}^n) - \tau^2\delta^n_{\mathbf{E}},
\end{aligned} \tag{5.13}
$$

with remainders

$$
\delta^n_{\mathbf{U}} = \int_{t_n}^{t_{n+1}} \frac{(t - t_n)(t_{n+1} - t)}{2\tau^2}\partial_t^3\mathbf{U}(t)\, dt, \qquad \mathbf{U} \in \{\mathbf{H}, \mathbf{E}\}. \tag{5.14}
$$

Obviously, they satisfy (5.9). Projecting Maxwell's equations (2.6a), (2.6b) onto V_h and applying the consistency property (2.23) we obtain

$$
\pi_h(\partial_t\mathbf{H}) = -\boldsymbol{\mathcal{C}}_{\mathbf{E}}\mathbf{E}, \qquad \pi_h(\partial_t\mathbf{E}) = \boldsymbol{\mathcal{C}}_{\mathbf{H}}\mathbf{H} - \mathbf{J}_h, \tag{5.15}
$$

so that the defects become

$$
\begin{aligned}
\mathbf{d}^n_{\mathbf{H}} &= \frac{\tau}{2}\boldsymbol{\mathcal{C}}_{\mathbf{E}}(\mathbf{e}^{n+1}_{\pi,\mathbf{E}} + \mathbf{e}^n_{\pi,\mathbf{E}}) + \tau^2\pi_h\delta^n_{\mathbf{H}}, \\
\mathbf{d}^n_{\mathbf{E}} &= -\frac{\tau}{2}\boldsymbol{\mathcal{C}}_{\mathbf{H}}(\mathbf{e}^{n+1}_{\pi,\mathbf{H}} + \mathbf{e}^n_{\pi,\mathbf{H}}) + \tau^2\pi_h\delta^n_{\mathbf{E}} + \frac{\tau^2}{4}\boldsymbol{\mathcal{C}}^e_{\mathbf{H}}\boldsymbol{\mathcal{C}}^e_{\mathbf{E}}\pi_h(\mathbf{E}^{n+1} - \mathbf{E}^n).
\end{aligned} \tag{5.16}
$$

The first term in the bound on the projection errors (5.8) follows with (5.5). For the defect $\mathbf{d}^n_{\mathbf{E}}$ we use (2.23) to write

$$
\boldsymbol{\mathcal{C}}_{\mathbf{E}}(\mathbf{E}^{n+1} - \mathbf{E}^n) = \pi_h\mathcal{C}_{\mathbf{E}}(\mathbf{E}^{n+1} - \mathbf{E}^n) = \int_{t_n}^{t_{n+1}} \pi_h\mathcal{C}_{\mathbf{E}}(\partial_t\mathbf{E}(t))\, dt = -\pi_h\Delta^n_{\mathbf{H}}.
$$

Here, the last equation follows with (2.6a). Applying $\boldsymbol{\mathcal{C}}^e_{\mathbf{H}}$ on both sides we end up with

$$
\boldsymbol{\mathcal{C}}^e_{\mathbf{H}}\boldsymbol{\mathcal{C}}^e_{\mathbf{E}}\pi_h(\mathbf{E}^{n+1} - \mathbf{E}^n) = -\boldsymbol{\mathcal{C}}^e_{\mathbf{H}}\pi_h\Delta^n_{\mathbf{H}} - \boldsymbol{\mathcal{C}}^e_{\mathbf{H}}\boldsymbol{\mathcal{C}}^e_{\mathbf{E}}(\mathbf{e}^{n+1}_{\pi,\mathbf{E}} - \mathbf{e}^n_{\pi,\mathbf{E}}) \tag{5.17}
$$

since $\boldsymbol{\mathcal{C}}^e_{\mathbf{H}}\boldsymbol{\mathcal{C}}_{\mathbf{E}} = \boldsymbol{\mathcal{C}}^e_{\mathbf{H}}\boldsymbol{\mathcal{C}}^e_{\mathbf{E}}$, see (2.34b). The second term in the bound (5.8) is then obtained by using Theorem 2.8, the CFL condition (4.1), and subsequently applying (5.4b). ∎

Assume that the CFL condition (4.1) is satisfied. Then, we can solve the error recursion (5.6) for $\mathbf{e}_h^{n+1}$:

$$
\mathbf{e}_h^{n+1} = \boldsymbol{\mathcal{R}}\mathbf{e}_h^n + \boldsymbol{\mathcal{R}}_L^{-1}\mathbf{d}^n. \tag{5.18}
$$

Since $\mathbf{e}_h^0 = 0$ we have

$$
\mathbf{e}_h^{n+1} = \sum_{m=0}^{n} \boldsymbol{\mathcal{R}}^{n-m}\boldsymbol{\mathcal{R}}_L^{-1}\mathbf{d}^m. \tag{5.19}
$$

Because of Lemmas 4.1 and 4.2 it is sufficient to prove the bound $\|\mathbf{d}^m\| \leq C\tau(h_{\max}^k + \tau^2)$. By (5.8) and (5.9) this bound holds for all terms except for $\frac{\tau^2}{4}\boldsymbol{\mathcal{C}}_{\mathbf{H}}^e \pi_h \Delta_{\mathbf{H}}^n$. Unfortunately, a naive bound on this term based on Theorem 2.8 and the CFL condition only yields a suboptimal bound of order $C\tau(h_{\max}^k + \tau)$. By (2.38) this bound can be improved to $C\tau(h_{\max}^k + \tau^{3/2})$ if we assume more regularity for $\partial_t^2 \mathbf{H}$. However, to obtain full order two in τ, we have to investigate the defects $\mathbf{d}^m$ more carefully.

From $\boldsymbol{\mathcal{C}}_{\mathbf{H}}^e = \boldsymbol{\mathcal{C}}_{\mathbf{H}} \circ \chi_e$ we have

$$\begin{pmatrix} 0 \\ -\tau \boldsymbol{\mathcal{C}}_{\mathbf{H}}^e \mathbf{U}_h \end{pmatrix} = \begin{pmatrix} 0 & \tau \boldsymbol{\mathcal{C}}_{\mathbf{E}} \\ -\tau \boldsymbol{\mathcal{C}}_{\mathbf{H}} & 0 \end{pmatrix} \begin{pmatrix} \chi_e \mathbf{U}_h \\ 0 \end{pmatrix} = (\boldsymbol{\mathcal{R}}_L - \boldsymbol{\mathcal{R}}_R) \begin{pmatrix} \chi_e \mathbf{U}_h \\ 0 \end{pmatrix} \tag{5.20}$$

for all $\mathbf{U}_h \in V_h$. Thus, we can split the defect $\mathbf{d}^n$ into

$$\mathbf{d}^n = \eta^n + (\boldsymbol{\mathcal{R}}_L - \boldsymbol{\mathcal{R}}_R)\xi^n, \tag{5.21a}$$

where

$$\eta^n = \mathbf{d}_\pi^n + \tau^2 \pi_h \delta^n, \qquad \xi^n = \begin{pmatrix} \xi_{\mathbf{H}}^n \\ \xi_{\mathbf{E}}^n \end{pmatrix} = \frac{\tau}{4} \begin{pmatrix} \chi_e \pi_h \Delta_{\mathbf{H}}^n \\ 0 \end{pmatrix}. \tag{5.21b}$$

Employing this splitting in (5.19) we obtain

$$\mathbf{e}_h^{n+1} = \xi^n - \boldsymbol{\mathcal{R}}^{n+1}\xi^0 + \sum_{m=0}^{n} \boldsymbol{\mathcal{R}}^{n-m} \boldsymbol{\mathcal{R}}_L^{-1} \eta^m - \sum_{m=0}^{n-1} \boldsymbol{\mathcal{R}}^{n-m}(\xi^{m+1} - \xi^m). \tag{5.22}$$

Note that

$$\xi_{\mathbf{H}}^{m+1} - \xi_{\mathbf{H}}^m = \frac{\tau}{4} \chi_e \pi_h \big(\partial_t \mathbf{H}^{m+2} - 2\partial_t \mathbf{H}^{m+1} + \partial_t \mathbf{H}^m\big).$$

Taylor expansion of $\partial_t \mathbf{H}^{m+1}$ at t_m and t_{m+2}, respectively, yields

$$\xi_{\mathbf{H}}^{m+1} - \xi_{\mathbf{H}}^m = \frac{\tau^2}{4} \int_{t_m}^{t_{m+2}} \left(1 - \frac{|t_{m+1} - t|}{\tau}\right) \chi_e \pi_h \big(\partial_t^3 \mathbf{H}(t)\big)\, dt. \tag{5.23}$$

It is easy to see that

$$\|\xi^{n+1} - \xi^n\|_{\mu \times \varepsilon} \leq \frac{\tau^2}{4} \int_{t_m}^{t_{m+2}} \|\partial_t^3 \mathbf{H}(t)\|_{\mu, \mathcal{T}_{h,c}}\, dt. \tag{5.24}$$

Now we have all ingredients to prove our main result.

THEOREM 5.2. *Let* $\mathbf{u} \in C\big(0, T; D(\mathcal{C}) \cap H^{k+1}(\mathcal{T}_h)^6\big) \cap C^3\big(0, T; L^2(\Omega)^6\big)$ *be the exact solution of* (2.6)*. Furthermore, assume that the CFL condition* (4.1) *is satisfied and that* $n\tau < T$*. Then, the error of the dG discretization and the locally implicit scheme* (3.6) *satisfies*

$$\|\mathbf{u}(t_n) - \mathbf{u}_h^n\|_{\mu \times \varepsilon} \leq C\Big(h_{\max}^k + \tau^2\Big). \tag{5.25}$$

More precisely, we have

$$
\begin{aligned}
\|\mathbf{u}(t_n) - \mathbf{u}_h^n\|_{\mu\times\varepsilon} \le & C_{\mathrm{app}} \left(\sum_{K\in\mathcal{T}_h} h_K^{2k+2} |\mathbf{u}(t_n)|_{k+1,K}^2 \right)^{1/2} \\
& + C_{\mathrm{stb}}^{3/2} C_\pi \tau \sum_{m=0}^{n-1} \frac{1}{2} \left(\sum_{K\in\mathcal{T}_h} h_K^{2k} |\mathbf{u}(t_{m+1}) + \mathbf{u}(t_m)|_{k+1,K}^2 \right)^{1/2} \\
& + C_{\mathrm{stb}}^{3/2} C_{\pi,c} \tau \sum_{m=0}^{n-1} \frac{1}{2} \left(\sum_{K\in\mathcal{T}_h} h_K^{2k} |\mathbf{E}(t_{m+1}) - \mathbf{E}(t_m)|_{k+1,K}^2 \right)^{1/2} \\
& + \frac{\tau^2}{4} \left(\max_{t\in[t_{n-1},t_n]} \|\partial_t^2 \mathbf{H}(t)\|_{\mu,\mathcal{T}_{h,c}} + C_{\mathrm{stb}}^{1/2} \max_{t\in[0,\tau]} \|\partial_t^2 \mathbf{H}(t)\|_{\mu,\mathcal{T}_{h,c}} \right) \\
& + \frac{1}{8} C_{\mathrm{stb}}^{3/2} \tau^2 \int_0^{t_n} \|\partial_t^3 \mathbf{u}(t)\|_{\mu\times\varepsilon} \, dt \\
& + \frac{1}{2} C_{\mathrm{stb}}^{1/2} \tau^2 \int_0^{t_n} \|\partial_t^3 \mathbf{H}(t)\|_{\mu,\mathcal{T}_{h,c}} \, dt.
\end{aligned} \tag{5.26}
$$

Proof. From the error splitting (5.2) and the triangle inequality we obtain

$$
\|\mathbf{e}^n\|_{\mu\times\varepsilon} \le \|\mathbf{e}_\pi^n\|_{\mu\times\varepsilon} + \|\mathbf{e}_h^n\|_{\mu\times\varepsilon}. \tag{5.27}
$$

The projection error $\mathbf{e}_\pi^n$ can be bounded with (5.3a). Thus, it remains to bound $\mathbf{e}_h^n$. This error satisfies the recursion (5.22) and thus by using the triangle inequality and Lemmas 4.1, 4.2 we infer

$$
\begin{aligned}
\|\mathbf{e}_h^n\|_{\mu\times\varepsilon} \le & \|\xi^{n-1}\|_{\mu\times\varepsilon} + C_{\mathrm{stb}}^{1/2} \|\xi^0\|_{\mu\times\varepsilon} \\
& + C_{\mathrm{stb}}^{3/2} \sum_{m=0}^{n-1} \|\eta^m\|_{\mu\times\varepsilon} + C_{\mathrm{stb}}^{1/2} \sum_{m=0}^{n-2} \|\xi^{m+1} - \xi^m\|_{\mu\times\varepsilon}.
\end{aligned}
$$

Inserting the bounds (5.8), (5.9), and (5.24) into the last two terms and observing that the first two terms can be bounded by

$$
\|\xi^{n-1}\|_{\mu\times\varepsilon} \le \frac{\tau^2}{4} \max_{t\in[t_{n-1},t_n]} \|\partial_t^2 \mathbf{H}(t)\|_{\mu,\mathcal{T}_{h,c}}, \qquad \|\xi^0\|_{\mu\times\varepsilon} \le \frac{\tau^2}{4} \max_{t\in[0,\tau]} \|\partial_t^2 \mathbf{H}(t)\|_{\mu,\mathcal{T}_{h,c}},
$$

concludes the proof. ∎

6. Numerical examples. In this section we verify our theoretical results by numerical examples. As test problem we consider the transverse magnetic (TM) polarization of Maxwell's equations in a homogeneous medium with $\mu = \varepsilon = 1$ in a square domain $\Omega = (-1,1)^2 \subset \mathbb{R}^2$,

$$
\begin{aligned}
\partial_t \mathbf{H}_x(t) &= -\partial_y \mathbf{E}_z(t), \\
\partial_t \mathbf{H}_y(t) &= \partial_x \mathbf{E}_z(t), \\
\partial_t \mathbf{E}_z(t) &= -\partial_y \mathbf{H}_x(t) + \partial_x \mathbf{H}_y(t) - \mathbf{J}_z(t), \\
\mathbf{H}_x(0) = \mathbf{H}_x^0, &\quad \mathbf{H}_y(0) = \mathbf{H}_y^0, \quad \mathbf{E}_z(0) = \mathbf{E}_z^0.
\end{aligned} \tag{6.1}
$$

As reference example we use

$$
\begin{aligned}
\mathbf{H}_x(t) &= -\pi \sin(\pi x) \cos(\pi y) e^t, \\
\mathbf{H}_y(t) &= \pi \cos(\pi x) \sin(\pi y) e^t, \\
\mathbf{E}_z(t) &= \sin(\pi x) \sin(\pi y) e^t,
\end{aligned} \tag{6.2a}
$$

mesh level	$h_{\max}$	$h_{\min}$	factor
1	0.239	0.0371	-
2	0.124	0.0294	0.79
3	0.0679	0.0272	0.93
4	0.0361	0.0236	0.87

(a) Mesh levels: Maximal and minimal diameter of the elements in the coarse part of the mesh.

inner level	$h_{\max}$	$h_{\min}$	factor
I	0.025	0.0125	-
II	0.025	0.00625	0.5
III	0.025	0.003125	0.5
IV	0.025	0.0015625	0.5

(b) Inner levels: Maximal and minimal diameter of the elements in the fine part of the mesh.

Table 1: Mesh parameters.

mesh level	max. stable τ	factor
1	0.0096	–
2	0.0078	0.81
3	0.0068	0.87
4	0.0059	0.87

(a) Locally implicit method, valid for all inner levels.

inner level	max. stable τ	factor
I	0.00276	-
II	0.00138	0.5
III	0.00069	0.5
IV	0.00035	0.5

(b) Verlet method, valid for all mesh levels.

Table 2: Maximal stable time steps.

which satisfy Maxwell's equation (6.1) with source term

$$\mathbf{J}_z(t) = -(1+2\pi^2)\sin(\pi x)\sin(\pi y)e^t. \tag{6.2b}$$

We use the following family of unstructured grids[1]: We start from the initial mesh shown in Figure 1a. The fine part of the mesh consists of the elements in the green marked square $[-0.05, 0.05]^2$. We then refine the mesh in two different ways. The first one is to refine the coarse part (outside of the green square), cf. Table 1a for the mesh parameters of the mesh levels 1–4 and Figure 1b for a plot of the mesh level 4. For the second one we refine the fine part of the mesh inside of the green square, cf. Figure 1c and Table 1b (inner levels I–IV).

We start by validating the CFL condition. The dependence on the mesh sizes is illustrated in Table 2a for the locally implicit scheme and in Table 2b for the Verlet method. The results clearly confirm that the CFL condition of the locally implicit method is independent of the inner levels but depends only on the refinement of the coarse (explicitly treated) part. Since the Verlet method is fully explicit its CFL condition depends on the inner levels.

Next, we show that spatial error is not affected by the splitting of the curl operators. This is illustrated by using a time step small enough such that the spatial error dominates. The results for $\tau = 2^{-15}$ and at the final time $T = 1$ are shown Figure 2.

Last, we verify the temporal convergence. We use polynomial degree $k = 5$ so that the time integration error dominates the spatial error. The final time is again $T = 1$. The graph of errors is given in Figure 3.

[1]The mesh data is available at http://www.waves.kit.edu/downloads/TR_15-1_data.zip.

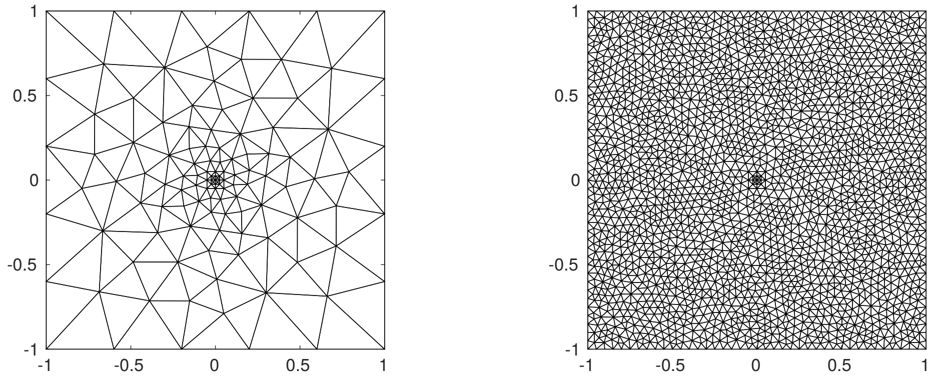

(a) Mesh level 1, inner level I.

(b) Mesh level 4, inner level I.

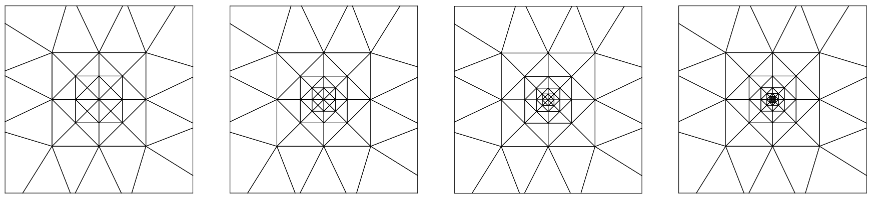

(c) Refinement of inner levels: From left to right inner levels I–IV.

Fig. 1: Illustration of two types of mesh refinements.

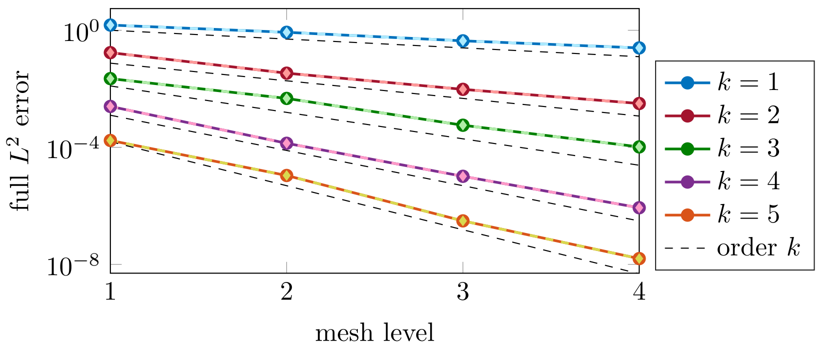

Fig. 2: Spatial errors with time step $\tau = 2^{-15}$ and different polynomial degrees for inner level I (solid) and inner level IV (dashed).

7. Concluding remarks. In this paper we have generalized a locally implicit time integration method initially proposed by Verwer [15] (for the ode resulting from spatial discretization) to the variational formulation of the central fluxes dG space discretization of linear Maxwell's equations. We showed how the operators emanating from space discretization have to be split in order to result in a locally implicit time integration scheme having a CFL condition which solely depends on the coarse part of the mesh. Furthermore, under this CFL condition we presented a rigorous stability and error analysis showing convergence of order two in time and k in space independent

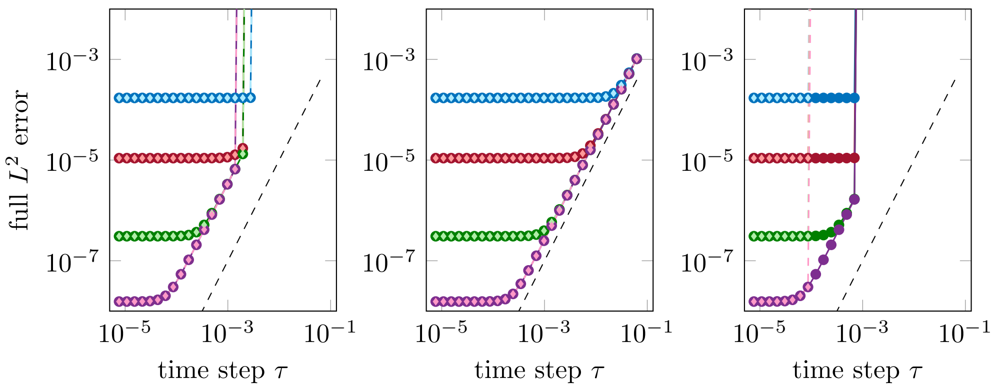

(a) Locally implicit (b) Crank–Nicolson (c) Verlet

Fig. 3: Temporal convergence with polynomial degree $k = 5$. Mesh levels 1 (blue), 2 (red), 3 (green), 4 (purple). Inner level I (solid), inner level IV (dashed). Black dashed line slope $\tau^2/10$.

of the fine part of the mesh. In addition, we provided numerical examples confirming the theoretical results.

Details on the efficient implementation and run time comparisons with other methods exploiting the local refinement in a small part of the mesh is ongoing work and will be presented elsewhere.

Acknowledgment. We thank Jonas Köhler for his careful reading of this manuscript.

Appendix A. Proofs postponed from Section 2.

Proof of Lemma 2.2. Integration by parts yields

$$\begin{aligned}(\mathcal{C}_{\mathbf{E}}\mathbf{E}_h, \mathbf{H}_h)_\mu = &\sum_{K\in\mathcal{T}_h} (\mathbf{E}_h, \operatorname{curl}\mathbf{H}_h)_K + \sum_{F\in\mathcal{F}_h^{\mathrm{int}}} \left(n_F \times [\![\mathbf{E}_h]\!]_F, \{\!\{\mathbf{H}_h\}\!\}_F^{\mu c}\right)_F \\ &+ \sum_{F\in\mathcal{F}_h^{\mathrm{int}}} \Big(\left(n_F \times \mathbf{E}_h|_K, \mathbf{H}_h|_K\right)_F - \left(n_F \times \mathbf{E}_h|_{K_F}, \mathbf{H}_h|_{K_F}\right)_F \Big).\end{aligned}$$

Using

$$\frac{\mu_K c_K}{\mu_K c_K + \mu_{K_F} c_{K_F}} = \frac{\varepsilon_{K_F} c_{K_F}}{\varepsilon_K c_K + \varepsilon_{K_F} c_{K_F}}, \qquad \frac{\mu_{K_F} c_{K_F}}{\mu_K c_K + \mu_{K_F} c_{K_F}} = \frac{\varepsilon_K c_K}{\varepsilon_K c_K + \varepsilon_{K_F} c_{K_F}}$$

we have

$$\begin{aligned}\left(n_F \times \mathbf{E}_h|_K, \mathbf{H}_h|_K\right)_F - &\left(n_F \times \mathbf{E}_h|_{K_F}, \mathbf{H}_h|_{K_F}\right)_F \\ &= \left(n_F \times [\![\mathbf{H}_h]\!]_F, \{\!\{\mathbf{E}_h\}\!\}_F^{\varepsilon c}\right)_F - \left(n_F \times [\![\mathbf{E}_h]\!]_F, \{\!\{\mathbf{H}_h\}\!\}_F^{\mu c}\right)_F ,\end{aligned}$$

which already yields the result. □

Proof of Theorem 2.8. We start with the proof of (2.35a). For $\mathbf{H}_h, \psi_h \in V_h$ we have by (2.21a) and (2.33)

$$(\mathcal{C}_{\mathbf{H}}^e \mathbf{H}_h, \psi_h)_\varepsilon = \sum_{K\in\mathcal{T}_{h,e}} (\operatorname{curl}\mathbf{H}_h, \psi_h)_K + \sum_{F\in\mathcal{F}_{h,c}^{\mathrm{int}}} \left(n_F \times [\![\chi_e \mathbf{H}_h]\!]_F, \{\!\{\psi_h\}\!\}_F^{\varepsilon c}\right)_F. \tag{A.1}$$

The first term in (A.1) can be bounded by using the Cauchy–Schwarz inequality and (2.31):

$$\begin{aligned}\sum_{K\in\mathcal{T}_{h,e}}\big(\operatorname{curl}\mathbf{H}_h,\psi_h\big)_K &\le C_{\mathrm{inv},c}\sum_{K\in\mathcal{T}_{h,e}} h_K^{-1}\|\mathbf{H}_h\|_K\|\psi_h\|_K\\ &= C_{\mathrm{inv},c}\sum_{K\in\mathcal{T}_{h,e}} c_K h_K^{-1}\|\mathbf{H}_h\|_{\mu,K}\|\psi_h\|_{\varepsilon,K}\\ &\le C_{\mathrm{inv},c}c_{\infty,c}\|\psi_h\|_{\varepsilon,\mathcal{T}_{h,e}}\Bigg(\sum_{K\in\mathcal{T}_{h,e}} h_K^{-2}\|\mathbf{H}_h\|^2_{\mu,K}\Bigg)^{1/2}.\end{aligned} \tag{A.2}$$

The second term in (A.1) is bounded as follows: First we use the Cauchy–Schwarz inequality and that n_F is a unit vector to obtain

$$\begin{aligned}&\sum_{F\in\mathcal{F}^{\mathrm{int}}_{h,c}}\big(n_F\times[\![\chi_e\mathbf{H}_h]\!]_F,\{\!\{\psi_h\}\!\}^{\varepsilon c}_F\big)_F\\ &\le\Bigg(\sum_{F\in\mathcal{F}^{\mathrm{int}}_{h,c}}\omega_F^{-1}\|[\![\chi_e\mathbf{H}_h]\!]_F\|_F^2\Bigg)^{1/2}\Bigg(\sum_{F\in\mathcal{F}^{\mathrm{int}}_{h,c}}\omega_F\|\{\!\{\psi_h\}\!\}^{\varepsilon c}_F\|_F^2\Bigg)^{1/2},\end{aligned} \tag{A.3}$$

for weights $\omega_F>0$ which will be chosen later. Next, we apply the triangle inequality, Young's inequality and the trace inequality (2.32). For the terms in the first sum this yields

$$\begin{aligned}\|[\![\chi_e\mathbf{H}_h]\!]_F\|_F^2 &\le 2C^2_{\mathrm{tr},c}\Big(h_K^{-1}\|\chi_e\mathbf{H}_h\|_K^2+h_{K_F}^{-1}\|\chi_e\mathbf{H}_h\|^2_{K_F}\Big)\\ &= 2C^2_{\mathrm{tr},c}\Big(\varepsilon_K c_K^2 h_K^{-1}\|\chi_e\mathbf{H}_h\|^2_{\mu,K}+\varepsilon_{K_F}c_{K_F}^2 h_{K_F}^{-1}\|\chi_e\mathbf{H}_h\|^2_{\mu,K_F}\Big),\end{aligned} \tag{A.4}$$

and for the second sum

$$\|\{\!\{\psi_h\}\!\}^{\varepsilon c}_F\|_F^2\le\frac{2C^2_{\mathrm{tr},c}}{\varepsilon_K c_K+\varepsilon_{K_F}c_{K_F}}\Big(c_K h_K^{-1}\|\psi_h\|^2_{\varepsilon,K}+c_{K_F}h_{K_F}^{-1}\|\psi_h\|^2_{\varepsilon,K_F}\Big), \tag{A.5}$$

where we used

$$\frac{\varepsilon_K c_K}{\varepsilon_K c_K+\varepsilon_{K_F}c_{K_F}}\le 1,\qquad \frac{\varepsilon_{K_F} c_{K_F}}{\varepsilon_K c_K+\varepsilon_{K_F}c_{K_F}}\le 1. \tag{A.6}$$

Now, we choose the weight

$$\omega_F=\frac{1}{2}(h_K+h_{K_F})(\varepsilon_K c_K+\varepsilon_{K_F}c_{K_F})$$

and use (2.30b) and (A.6) in (A.4) to obtain

$$\omega_F^{-1}\|[\![\chi_e\mathbf{H}_h]\!]_F\|_F^2\le 2C^2_{\mathrm{tr},c}\rho_c\big(c_K h_K^{-2}\|\chi_e\mathbf{H}_h\|^2_{\mu,K}+c_{K_F}h_{K_F}^{-2}\|\chi_e\mathbf{H}_h\|^2_{\mu,K_F}\big), \tag{A.7}$$

and (2.30b) in (A.5) to infer

$$\omega_F\|\{\!\{\psi_h\}\!\}^{\varepsilon c}_F\|_F^2\le 2C^2_{\mathrm{tr},c}\rho_c\big(c_K\|\psi_h\|^2_{\varepsilon,K}+c_{K_F}\|\psi_h\|^2_{\varepsilon,K_F}\big). \tag{A.8}$$

Inserting (A.7) and (A.8) in (A.3) and using the bound N_∂ on the number of mesh faces composing an element boundary we conclude

$$\begin{aligned}
&\sum_{F\in\mathcal{F}_{h,c}^{\mathrm{int}}} \big(n_F\times[\![\chi_e\mathbf{H}_h]\!]_F, \{\!\{\psi_h\}\!\}_F^{\varepsilon c}\big)_F \\
&\le \widehat{C}N_\partial \Bigg(\sum_{K\in\mathcal{T}_{h,e}\cup\mathcal{T}_{h,ci}} c_K h_K^{-2}\|\chi_e\mathbf{H}_h\|_{\mu,K}^2\Bigg)^{1/2} \Bigg(\sum_{K\in\mathcal{T}_{h,e}\cup\mathcal{T}_{h,ci}} c_K\|\psi_h\|_{\varepsilon,K}^2\Bigg)^{1/2} \qquad \text{(A.9)}\\
&\le \widehat{C}N_\partial c_{\infty,c}\|\psi_h\|_{\varepsilon,\mathcal{T}_{h,e}\cup\mathcal{T}_{h,ci}} \Bigg(\sum_{K\in\mathcal{T}_{h,e}} h_K^{-2}\|\mathbf{H}_h\|_{\mu,K}^2\Bigg)^{1/2},
\end{aligned}$$

where we abbreviated $\widehat{C} = 2C_{\mathrm{tr},c}^2\rho_c$. The assertion (2.35a) is then obtained by applying (A.2) and (A.9) in (A.1) and using the identity

$$\|\mathcal{C}_{\mathbf{H}}^e\mathbf{H}_h\|_\varepsilon = \sup_{\psi_h\in V_h,\|\psi_h\|_\varepsilon=1} \big(\mathcal{C}_{\mathbf{H}}^e\mathbf{H}_h,\psi_h\big)_\varepsilon. \qquad \text{(A.10)}$$

The result (2.35b) is obtained analogously. ☐

Proof of Lemma 2.9. Let K_e and K_i denote the explicit and implicit element corresponding to a face $F\in\mathcal{F}_{h,ci}^{\mathrm{int}}$. Employing $\mathbf{H}\in D(\mathcal{C}_{\mathbf{H}})\cap H^1(\mathcal{T}_h)^3$ and $\psi_h\in V_h$ in (A.1) and exploiting (2.22) we have

$$\big(\mathcal{C}_{\mathbf{H}}^e\mathbf{H},\psi_h\big)_\varepsilon = \sum_{K\in\mathcal{T}_{h,e}} \big(\operatorname{curl}\mathbf{H},\psi_h\big)_K + \sum_{F\in\mathcal{F}_{h,ci}^{\mathrm{int}}} \big(n_F\times\mathbf{H}|_{K_e},\{\!\{\psi_h\}\!\}_F^{\varepsilon c}\big)_F.$$

For the first term we use the Cauchy–Schwarz inequality and the assumption on the coefficients (2.5) to obtain

$$\sum_{K\in\mathcal{T}_{h,e}} \big(\operatorname{curl}\mathbf{H},\psi_h\big)_K \le \varepsilon_0^{-1/2}\|\operatorname{curl}\mathbf{H}\|_{\mathcal{T}_{h,e}}\|\psi_h\|_{\varepsilon,\mathcal{T}_{h,e}}. \qquad \text{(A.11)}$$

For the second term we use the Cauchy–Schwarz inequality, (A.6) and that n_F is a unit vector to show

$$\begin{aligned}
&\sum_{F\in\mathcal{F}_{h,ci}^{\mathrm{int}}} \big(n_F\times\mathbf{H}|_{K_e},\{\!\{\psi_h\}\!\}_F^{\varepsilon c}\big)_F \\
&\qquad\le \Bigg(\sum_{F\in\mathcal{F}_{h,ci}^{\mathrm{int}}} \omega_F^{-1}\|\mathbf{H}|_{K_e}\|_F^2\Bigg)^{1/2} \Bigg(\sum_{F\in\mathcal{F}_{h,ci}^{\mathrm{int}}} \omega_F\big(\|\psi_h|_{K_e}\|_F+\|\psi_h|_{K_i}\|_F\big)^2\Bigg)^{1/2}
\end{aligned}$$

with weight $\omega_F = (h_{K_e}+h_{K_i})/2$. For the first term we first apply the continuous trace inequality [4, Section 1.1.3] and subsequently (2.30b)

$$\omega_F^{-1}\|\mathbf{H}|_{K_e}\|_F^2 \le C_{\mathrm{ctr,c}}^2\omega_F^{-1}\|\mathbf{H}_h\|_{1,K_e}^2 \le C_{\mathrm{ctr,c}}^2\rho_c h_{K_e}^{-1}\|\mathbf{H}_h\|_{1,K_e}^2. \qquad \text{(A.12)}$$

For the second term we use Young's inequality and the trace inequality (2.32) to infer

$$\begin{aligned}
\omega_F\big(\|\psi_h|_{K_e}\|_F+\|\psi_h|_{K_i}\|_F\big)^2 &\le 2C_{\mathrm{tr},c}^2\omega_F\big(h_{K_e}^{-1}\|\psi_h\|_{K_e}^2 + h_{K_i}^{-1}\|\psi_h\|_{K_i}^2\big)\\
&\le 2C_{\mathrm{tr},c}^2\rho_c\varepsilon_0^{-1}\big(\|\psi_h\|_{\varepsilon,K_e}^2+\|\psi_h\|_{\varepsilon,K_i}^2\big).
\end{aligned}$$

Here, the second inequality is obtained from (2.30b) and (2.5). Thus, we have

$$\sum_{F \in \mathcal{F}_{h,ci}^{\mathrm{int}}} \left(n_F \times \mathbf{H}|_{K_e}, \{\!\{\psi_h\}\!\}_F^{\varepsilon c}\right)_F \leq C'_{\mathrm{bnd},c} \varepsilon_0^{-1/2} \|\psi_h\|_{\varepsilon,\mathcal{T}_{h,c}} \left(\sum_{F \in \mathcal{F}_{h,ci}^{\mathrm{int}}} h_{K_e}^{-1} \|\mathbf{H}\|_{1,K_e}^2 \right)^{1/2}.$$

Applying (A.10) gives the stated result. □

REFERENCES

[1] A. Demirel, J. Niegemann, K. Busch, and M. Hochbruck, *Efficient multiple time-stepping algorithms of higher order*, J. Comput. Phys., 285 (2015), pp. 133–148.

[2] S. Descombes, S. Lanteri, and L. Moya, *Locally implicit time integration strategies in a discontinuous Galerkin method for Maxwell's equations*, J. Sci. Comput., 56 (2013), pp. 190–218.

[3] ———, *Locally implicit discontinuous galerkin time domain method for electromagnetic wave propagation in dispersive media applied to numerical dosimetry in biological tissues*, Technical Report HAL Id: hal-01133694, INRIA, 2015.

[4] D. A. Di Pietro and A. Ern, *Mathematical aspects of discontinuous Galerkin methods*, vol. 69 of Mathématiques & Applications (Berlin) [Mathematics & Applications], Springer, Heidelberg, 2012.

[5] V. Dolean, H. Fahs, L. Fezoui, and S. Lanteri, *Locally implicit discontinuous Galerkin method for time domain electromagnetics*, J. Comput. Phys., 229 (2010), pp. 512–526.

[6] M. J. Grote, M. Mehlin, and T. Mitkova, *Runge-Kutta-based explicit local time-stepping methods for wave propagation*, SIAM J. Sci. Comput., 37 (2015), pp. A747–A775.

[7] M. J. Grote and T. Mitkova, *Explicit local time-stepping methods for Maxwell's equations*, J. Comput. Appl. Math., 234 (2010), pp. 3283–3302.

[8] ———, *High-order explicit local time-stepping methods for damped wave equations*, J. Comput. Appl. Math., 239 (2013), pp. 270–289.

[9] J. S. Hesthaven and T. Warburton, *Nodal discontinuous Galerkin methods*, vol. 54 of Texts in Applied Mathematics, Springer, New York, 2008. Algorithms, analysis, and applications.

[10] M. Hochbruck and T. Pažur, *Implicit Runge–Kutta methods and discontinuous Galerkin discretizations for linear Maxwell's equations*, SIAM J. Numer. Anal., 53 (2015), pp. 485–507.

[11] P. Monk, *Finite element methods for Maxwell's equations*, Numerical Mathematics and Scientific Computation, Oxford University Press, New York, 2003.

[12] L. Moya, *Temporal convergence of a locally implicit discontinuous Galerkin method for Maxwell's equations*, ESAIM Math. Model. Numer. Anal., 46 (2012), pp. 1225–1246.

[13] A. Pazy, *Semigroups of Linear Operators and Applications to Partial Differential Equations*, vol. 44 of Applied Mathematical Sciences, Springer, New York, 1983.

[14] S. Piperno, *Symplectic local time-stepping in non-dissipative DGTD methods applied to wave propagation problems*, M2AN Math. Model. Numer. Anal., 40 (2006), pp. 815–841 (2007).

[15] J. G. Verwer, *Component splitting for semi-discrete Maxwell equations*, BIT, 51 (2011), pp. 427–445.